Check for updates

METHOD ARTICLE

REVISED Oriented artificial nanofibers and laser induced periodic surface structures as substrates for Schwann cells alignment

[version 3; peer review: 2 approved, 1 approved with reservations]

Sebastian Lifka[1], Cristina Plamadeala[2], Agnes Weth[1], Johannes Heitz[2], Werner Baumgartner[1]

[1]Institute of Biomedical Mechatronics, Johannes Kepler University Linz, Linz, Upper Austria, 4040, Austria
[2]Institute of Applied Physics, Johannes Kepler University Linz, Linz, Upper Austria, 4040, Austria

v3 **First published:** 24 Apr 2024, **4**:80
https://doi.org/10.12688/openreseurope.17370.1
Second version: 20 Aug 2024, **4**:80
https://doi.org/10.12688/openreseurope.17370.2
Latest published: 22 Oct 2024, **4**:80
https://doi.org/10.12688/openreseurope.17370.3

Abstract

People with injuries to the peripheral nervous system suffer from paralysis of the facial muscles, fingers and hands or toes and feet, often for the rest of their lives, due to its poor functional regeneration. Therefore, to improve patients' quality of life, there is an urgent need for conduits that effectively support the healing of large defects in nerve pathways through specific guidance of nerve cells. This paper describes two specific methods for achieving directed growth of Schwann cells, a type of glial cells that can support the regeneration of the nerve pathway by guiding the neuronal axons in the direction of their alignment. One method uses aligned polyamide-6 (PA-6) nanofibers produced via electrospinning on a very fast rotating structured collector, which enables easy nanofiber detachment, without additional effort. The other method implies the exposure of a poly(ethylene terephthalate) (PET) foil to a KrF* laser beam, that renders a nanorippled surface topography. Schwann cell growth on these substrates was inspected after one week of cultivation by means of scanning electron microscopy (SEM). For both methods we show that Schwann cells grow in a certain direction, predetermined by nanofiber and nanoripple orientation. In contrast, cells cultivated on randomly oriented nanofibers or unstructured surfaces, show an omnidirectional growth behavior. These two methods can be used to produce nerve conduits for the treatment of injuries to the peripheral nervous system.

Open Peer Review

Approval Status ✓ ? ✓

	1	2	3
version 3 (revision) 22 Oct 2024			✓ view
version 2 (revision) 20 Aug 2024	✓ view		✗ view
version 1 24 Apr 2024	? view	? view	

1. **Harald Luksch**, Technische Universität München, Weihenstephan, Germany

2. **Sandra I. Vieira**, University of Aveiro, Aveiro, Portugal
Nathalie Barroca, University of Aveiro, Aveiro, Portugal

3. **Tak-Ho Chu**, University of Calgary, Calgary, Canada

Any reports and responses or comments on the article can be found at the end of the article.

Keywords
Aligned Nanofibers, Electrospinning, Nanoripples, Laser-Induced Periodic Surface Structures, Nerve Regeneration, Tissue Engineering, Schwann cells

This article is included in the Medical Biotechnology gateway.

This article is included in the Horizon 2020 gateway.

Corresponding authors: Sebastian Lifka (sebastian.lifka@jku.at), Cristina Plamadeala (cristina.plamadeala@jku.at)

Author roles: Lifka S: Conceptualization, Data Curation, Formal Analysis, Investigation, Methodology, Validation, Visualization, Writing – Original Draft Preparation; **Plamadeala C**: Conceptualization, Data Curation, Formal Analysis, Investigation, Methodology, Validation, Visualization, Writing – Original Draft Preparation; **Weth A**: Conceptualization, Data Curation, Formal Analysis, Investigation, Methodology, Resources, Validation, Visualization, Writing – Original Draft Preparation; **Heitz J**: Conceptualization, Funding Acquisition, Project Administration, Supervision, Writing – Review & Editing; **Baumgartner W**: Conceptualization, Funding Acquisition, Project Administration, Supervision, Writing – Review & Editing

Competing interests: No competing interests were disclosed.

Grant information: This project has received funding from the European Union's Horizon 2020 research and innovation programme under grant agreement No [862016] (Antiadhesive Bionic Combs for Handling of Nanofibers [BioCombs4Nanofibers]) and by the Austrian COMET-K2 program of the Linz Center of Mechatronics (LCM).
The funders had no role in study design, data collection and analysis, decision to publish, or preparation of the manuscript.

Copyright: © 2024 Lifka S *et al*. This is an open access article distributed under the terms of the Creative Commons Attribution License, which permits unrestricted use, distribution, and reproduction in any medium, provided the original work is properly cited.

How to cite this article: Lifka S, Plamadeala C, Weth A *et al.* **Oriented artificial nanofibers and laser induced periodic surface structures as substrates for Schwann cells alignment [version 3; peer review: 2 approved, 1 approved with reservations]** Open Research Europe 2024, **4**:80 https://doi.org/10.12688/openreseurope.17370.3

First published: 24 Apr 2024, **4**:80 https://doi.org/10.12688/openreseurope.17370.1

REVISED **Amendments from Version 2**

In this version we implement changes and improvements according to the comments and suggestions of Reviewer 3. Please find the changes made listed below:

- We made slight improvements on the Abstract.

- We added a brief literature review regarding current state and challenges of clinical nerve injury treatment.

- We clarified how these two methods can be implemented in a 3D configuration in nerve conduits.

- We added a quantification of the quality of the directionality of the aligned fibers and cells by introducing the standard deviation of the normal distribution fit of the histograms in Figure 5 and Figure 8.

- We justified why the 8 m/s nanofiber sample was used instead of the 14 m/s sample.

- We added information regarding the sample size for data analysis.

- A brief description of the staining method used for fluorescence microscopy was added to the supplement in the Zenodo repository.

- We discussed LIPSS formation on different materials.

- We added a Figure S4 to the supplementary material in the Zenodo repository showing oriented Schwann cells on an uncoated nanofiber sample. Furthermore, we explained in detail why we decided to coat the nanofiber samples with PLL.

- A brief discussion of increasing fiber diameter with increasing speed has been added.

- We described how the method can be adapted to biocompatible polymers.

- Last but not least, we have expanded the Conclusion slightly.

Any further responses from the reviewers can be found at the end of the article

Introduction

In the peripheral nervous system of vertebrates, neurons are responsible for receiving and transmitting electrical and chemical signals and glial cells provide the necessary support and protection for neurons. Here, the most important glial cells are Schwann cells. They are responsible for the creation of myelin sheaths that protect and insulate neuronal axons (Cattin *et al.*, 2015). They are also essential and indispensable for axon regeneration in the event of injury (Manganas *et al.*, 2022). The peripheral axons regenerate in regeneration tracks (i.e., bands of Büngner) formed by elongated Schwann cells (Jessen & Mirsky, 2019). Small gaps can regenerate on their own, while large gaps are considered to require the support of a nerve graft.

Today's gold standard in clinical treatment of nerve injuries are autografts for bridging large gaps. However, limitations like donor site morbidity and the need of a second surgery leave room for improvement. An alternative to nerve autografts are nerve allografts. Although these avoid the disadvantages of autografts mentioned above, they require immunotherapy for approximately 18 months to prevent rejection of the graft (Meena *et al.*, 2021). A third possibility for clinical treatment of large nerve injuries are artificial nerve conduits. Current commercially available conduits consist of simple hollow tubes connecting the two damaged nerve stumps and aim for increasing the number, speed, and length of the regenerating axons (Meena *et al.*, 2021). These conduits must exhibit adequate properties like biocompatibility, biodegradability, mechanical properties, and biochemical properties. The major challenges of nerve conduits are wrong target innervations and axonal dispersions, for example. Furthermore, their repair length is currently limited to less than 3 cm in humans (Meena *et al.*, 2021).

However, the currently available artificial nerve grafts have insufficient success rates, especially for large nerve gaps of several centimeter. A key factor here is the elongated orientation of the Schwann cells which is induced by stimuli from their surrounding either in the extra cellular matrix (ECM) or in case of artificial implants by the supporting material (Jiang *et al.*, 2024; Manganas *et al.*, 2022).

One possibility to guide Schwann cells would be the use of natural silk. (Millesi *et al.*, 2021) and (Stadlmayr *et al.*, 2024), for example, have recently conducted promising research into the use of natural spider silk in nerve regeneration. Since the harvesting of natural silk can be costly and time-consuming, the use of artificial fibers, such as nanofibers produced using the so-called electrospinning process, would be advantageous. As nanofiber materials for nerve guidance conduits, one could employ electrospun fibers from materials that are biocompatible and biodegradable (i.e., poly-ε-caprolactone or collagen/poly-ε-caprolactone blends). Results of an earlier activity in this direction are reported in (Schnell *et al.*, 2007). In the process of electrospinning, the fibers became oriented more or less parallel to each other as a suspended array between the two electrode bars. Under optimized conditions, for instance deposition on a drum or disc electrode with high-speed rotation (Chen *et al.*, 2021; Wang *et al.*, 2018), it is possible to produce, nanofiber mats with parallel orientation. Directed nanofibers have also been used as scaffolds in nerve regeneration. (Huang *et al.*, 2015) used directed cellulose acetate butyrate (CAB) nanofibers for the regeneration of nerves in rats.

However, the removal of the nanofiber non-woven from the electrodes or supporting materials without tearing remains problematic. To fill conduits with a larger lumen with parallel oriented fibers, the combination of 3D frames (i.e., a stair case like target) and supporting gels have already been tested in animal experiments (Kriebel *et al.*, 2017). Also, roll-up memory shape supports were considered (Wang *et al.*, 2020).

A second possibility to guide Schwann cells is to create a substrate with nanoripples, also known as laser-induced periodic surface structures (LIPSS), that can be achieved by short-pulsed laser processing (Bonse *et al.*, 2017). In previous work, we and others have investigated the effects of laser-induced nanostructures and hierarchical micro/nanostructures on adherent cells cultured thereon (Fosodeder *et al.*, 2020; Maalouf *et al.*, 2022; Muck *et al.*, 2021). Depending on the specific structure, cell adhesion, proliferation, or migration

can be inhibited, cell alignment can be induced for alignment, production of extra-cellular matrix proteins can be promoted, or the differentiation of stem cells into specific cell types can be supported. It has been shown, that laser-induced nanoripples and dual-rough hierarchical micro/nanostructures can be used to control Schwann cells attachment and migration, at least on silicon (Yiannakou *et al.*, 2017). However, to our knowledge no detailed investigations were performed so far with Schwann cells on laser-structured polymeric materials, which could be of relevance for nerve implants.

In this work we present two methods which can be used effectively in the future for the production of implants in nerve regeneration. One method enables the production of aligned nanofibers which can be easily detached from the electrospinning collector as an independent non-woven without additional coating or complex additional work, as it was the case up to now and thus significantly simplifies the manufacturing process. This is achieved by a collector rotating at a very high speed which winds up the electrospun fiber as if on a wire drum. The surface of the collector is structured with a special micro-surface structure, which has already been described in more detail in a previous publication (Lifka *et al.*, 2023). The surface structure allows the nanofiber non-woven to be removed from the collector easily and without leaving any residue. This supportless electrospinning technique makes a simple and easy production of nerve guides possible and is therefore the unique feature of this method. The other method describes the production of LIPSS, also known as nanoripples, which, due to their resemblance to the ECM, enable the aligned growth of nerve cells. This method is, however, limited to more or less rigid polymer foils (Plamadeala *et al.*, 2023; Rebollar *et al.*, 2008; Rebollar *et al.*, 2012) and is therefore only suitable to a limited extent for flexible nerve conduits. There are a few approaches to produce laser-induced nanoripples on very thin flexible polymer films (Buchberger *et al.*, 2024) or on bendable polymer microfibers (Sajzew *et al.*, 2015), but these are very delicate to handle. Therefore, the preferred method for the production of nerve conduits tends to be the method that uses nanofibers, as these have a high degree of flexibility. Nevertheless, we show for both methods that, in contrast to randomly oriented fibers or unstructured, flat surfaces, they promote oriented cell growth in a direction predefined by the orientation of the fibers and ripples. Both methods can be used for nerve conduit production, whether it is a surface structured polymer foil rolled up to a hollow tube, a thin and very flexible aligned nanofiber non-woven rolled up to a thin roll, or a combination of both, hence, a nanofiber roll wrapped in a thin PET film.

Methods

Aligned nanofibers

The most important and novel part of this method is the rotating collector whose surface contains a structure in the µm range. This structure has already been presented in a previous publication and consists in principle of a simple triangular geometry which forms a jagged surface structure. In (Lifka *et al.*, 2023), this structure was produced on a cylindrical collector with the aid of a thread turning tool in the form of a very fine thread, whereby the direction of preference of the structure is orthogonal to the collector axis. This variant represents the most unfavorable alignment of the structure for this application (the aligned nanofibers must be orthogonal to the direction of the structure in order to guarantee its function). Therefore, the structure must be manufactured in such a way that its orientation is parallel to the cylinder/collector axis. In the sense of simple, fast and cost-effective production, the triangular structure was produced by knurling the cylinder surface with axis-parallel grooves.

For this purpose, a cylindrical collector made of aluminum with a diameter of 40 mm was manufactured and machined on a lathe using a knurling wheel (ZEUS knurling wheel 11 AA 15 x 4 x 4 G7 T=0.3 PM a=90°, Article number: 41013392, Hommel+Keller Präzisionswerkzeuge GmbH, Aldingen, Germany) with the triangular surface structure. The structure therefore has a periodicity and depth of approximately 300 µm with a tip angle of 90°. To enable the collector to rotate, it is supported by two ball bearings (6001-2Z, SKF Österreich AG, Steyr, Austria) to the left and right of the structured surface. The bearing blocks were manufactured using a 3D printer (Photon Mono-X, Hongkong Anycubic Technology Co., Shenzen, China). The resin used for the 3D printed parts was the "Blu" resin from Siraya Tech (Blu-Tough Resin/Nylon Black, Siraya Tech, San Gabriel, California, USA). The collector is driven by a brushless DC motor (DB28M01, Nanotec Electronic GmbH & Co. KG, Feldkirchen, Germany) via a claw coupling (MJC19-4-A, JD12/19-85B; Ruland Manufacturing Co., Inc., Marlborough, UK). The maximum achievable rotational speed of the collector is approximately 14 meter per second. All CAD data and 2D drawing derivation required for the production of the collector are freely available in a Zenodo repository (Lifka *et al.*, 2024).

For electrospinning, the rotating drum collector assembly (Figure 1B) was mounted on a custom-made electrospinning setup, as shown in Figure 1A. The setup is based on the classic horizontal electrospinning process in which a polymer solution is conveyed evenly through a thin metal needle with the aid of a syringe pump and applied to a collector in the form of thin nanofibers with the use of a strong electric field. The setup consists of a basic frame made of aluminum profiles which enables precise adjustment of the needle-collector distance. The polymer solution is conveyed evenly through a thin metal needle (Sterican 21G x 7/8″ blunt, B. Braun SE, Melsungen, Germany) using a custom-made syringe pump. The necessary electric field is generated by a high-voltage generator (HCP 35-35,000, FuG Elektronik GmbH, Schechen, Germany). The needle is the positive electrode and the collector is the negative electrode. The needle is contacted directly via a crocodile clip, while the collector is contacted via the conductive ball bearings to avoid sliding contact. The polymer solution for the nanofibers consists of 15 wt.% polyamide-6 (PA-6) (provided by Elmarco s.r.o., Liberec, Czech Republic) dissolved in formic acid (FA) (ROTIPURAN® ≥98%, p.a., ACS, Art. No. 4724.1, Carl Roth GmbH + Co. KG.,

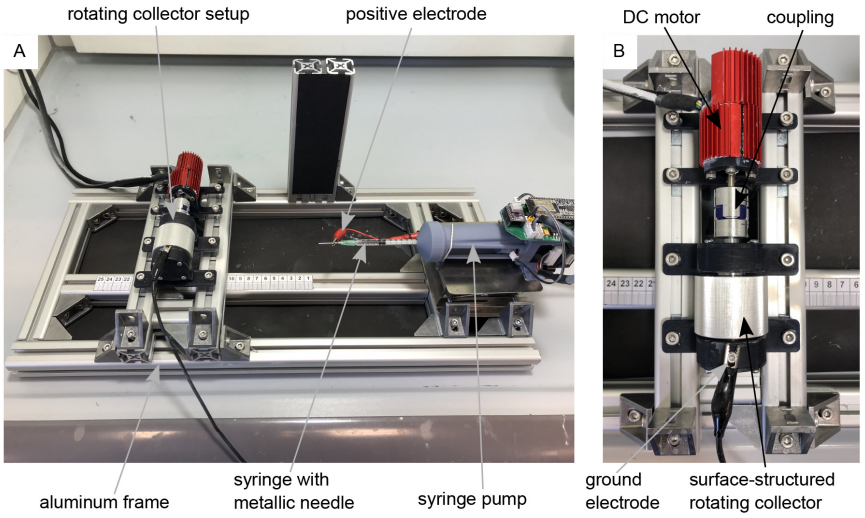

Figure 1. Electrospinning-setup for the production of aligned nanofibers. (**A**) Custom-made electrospinning setup. (**B**) Rotating drum collector setup mounted on the electrospinning setup.-

Karlsruhe, Germany), and acetic acid (AA) (ROTIPURAN 100%, p.a., Art. No. 3738.4, Carl Roth GmbH + Co. KG., Karlsruhe, Germany) in a (weight) ratio of 2:1. A total of 15 g of the polymer solution was prepared, for which 2.25 g PA-6, 4.25 g FA and 8.5 g AA were used. The parameters for the spinning process were selected as follows: Needle-collector distance of 13 cm, needle-collector voltage of 20 kV, and flow rate of 0.34 mLh^{-1}.

The motor speed was controlled and set via the software "Plug & Drive Studio 3" (v. 1.5.3.0, Nanotec Electronic GmbH & Co. KG, Feldkirchen, Germany). Various rotational speeds of the collector were tested until the fibers were oriented in the desired direction. The electrospinning process took about 10 minutes for each sample. After this time, a fleece that was thick and robust enough for further processing could be guaranteed. The finished non-woven was then cut open with a scalpel parallel to the collector axis and carefully removed from the collector with tweezers. Thanks to the surface structuring, the fleece could be removed easily and without leaving any residue. The Zenodo repository (Lifka *et al.*, 2024) contains a video (Non-Woven_Detachement_from_Collector.mkv) showing the removal process of the aligned nanofiber non-woven. The specimens of the nanofiber non-woven were then sputter-coated with gold (SCD 005, BAL-TEC Inc., Balzers, Liechtenstein) for 80 s with 21 mA and examined under a scanning electron microscope (SEM) (Philips 525, Philips Electron Optics, Amsterdam, The Netherlands). The SEM images subsequently serve as the basis for the analysis of the directionality and the average fiber diameter.

The statistical analyses of fiber directionality and fiber diameter were performed using ImageJ (v. 1.51w, Rasband, W.S., U. S. National Institutes of Health, Bethesda, Maryland, USA). The directionality analysis function (v2.3.0, method: Fourier components) was used to analyze the fiber orientation. The DiameterJ (v. 1-018) plug-in (Hotaling *et al.*, 2015) was used to analyze the fiber diameter. The corresponding diagrams were created with the help of Python-3 (v. 3.10.9, Python Software Foundation, Beaverton, Oregon, USA) and matplotlib (v. 3.3) (Hunter, 2007) from the .csv files generated by ImageJ. All underlying data can be found in the Zenodo repository (Lifka *et al.*, 2024).

Nanoripples

To produce ripples on poly(ethylene terephthalate) (PET) foils with a thickness of 50 µm (Goodfellow Ltd., Bad Nauheim, Germany), a KrF* (krypton fluoride) excimer laser (LPX 300, Lambda Physik, 181 Göttingen, Germany) was used, with a wavelength of 248 nm, 20 ns pulse duration, and 10 Hz pulse repetition rate. The setup is similar to the setup for laser processing of PET foils used in (Richter *et al.*, 2021) and is shown in Figure 2. Prior to exposure, the PET foils were rinsed with ethanol and thoroughly dried with nitrogen, in order to remove any debris. Later on, the foils were fixed onto the sample holder at a 30° incidence angle and exposed to 6000 pulses at an energy of 12.6 – 12.8 mJ, applying an average fluence of 10 mJ cm^{-2}. Laser beam energy was measured with a high-area high-damage energy sensor (J45LP-MUV, Coherent, Portland, United States) with the help of a laser energy meter (FieldMaxII-P™, Coherent, Portland, USA).

Scanning electron microscope (model REM 1540XB-Crossbeam, Zeiss, Oberkochen, Germany) images of nanoripples were acquired at ten different positions within the nanostructured area and analyzed by using the free software Gwyddion (v. 2.61, Czech _Metrology Institute, Brno, Czech Republic) in order to calculate the spatial period. The resulting average spatial period is $\Lambda = 331 \pm 11$ nm. The underlying data for spatial period calculation "Spatial period calculation.docx" can be found in the Zenodo repository (Lifka *et al.*, 2024). The height of the resulting nanoripples was determined in previous works to be approximately between 110 nm to 160 nm (Buchberger *et al.*, 2023; Heitz *et al.*, 2024).

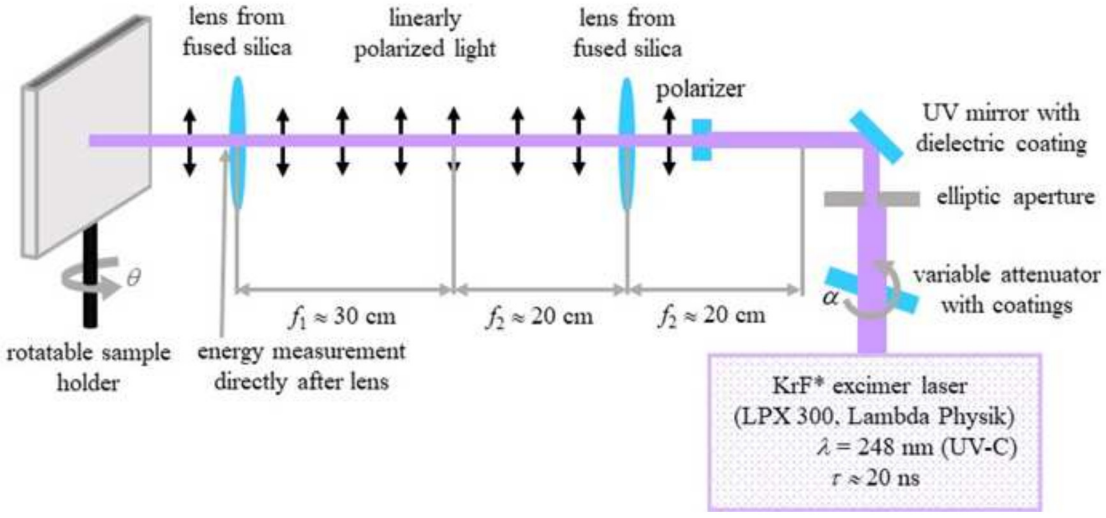

Figure 2. Setup for laser-induced periodic surface structures fabrication on poly(ethylene terephthalate) foils. (Reprinted from (Buchberger *et al.*, 2023) which is an open-access article distributed under the terms of the Creative Commons Attribution 4.0 International (CC-BY 4.0)).

Cell cultivation

To validate and show the oriented cell growth on samples produced with the above described methods, murine Schwann cells (Immortalized Mouse Schwann Cells (IMS32), T0295, Applied Biological Materials Inc., Richmond, Canada) were cultured for ten days in 4 mL grow medium consisting of PriGrow III (TM003, Applied Biological Materials Inc., Richmond, Canada) + 10% fetal bovine serum (FBS)(F7524, Sigma-Aldrich, St. Lois, Missouri, USA) + 1% Penicillin/ Streptomycin Solution (G255, Applied Biological Materials Inc., Richmond, Canada) at 37.0 °C and 5% CO_2 in an incubator (New Brunswick Galaxy® 48 S CO2, Eppendorf, Hamburg, Germany) on the corresponding sample. The medium was changed every two days. Prior to cell cultivation, samples were coated with a oly-L-lysine (PLL) hydrobromide (P9155, Sigma Aldrich, Sigma-Aldrich, St. Lois, Missouri, USA) solution at a concentration of 40 µg ml^{-1} in double-distilled water, incubated for 10 minutesat room temperature, then washed with distilled water, and finally air-dried at room temperature. The cell density upon seeding on the samples was 25,000 cells per cm^2 resulting in a total number of approximately 65,000 cells per sample.

Image manipulation

All images shown in the figures have been slightly manipulated to improve the clarity of the figures. The original, unmanipulated images can be found as underlying data in the Zenodo repository (Lifka *et al.*, 2024). The software used for image manipulation was on the one hand Corel Vector (v. 23.0.0.363, Alludo, Ottawa, Canada) and on the other hand Inkscape (v. 0.92.4, The Inkscape Project c/o Software Freedom Conservancy, Brooklyn, New York, USA). While Corel Vector is a proprietary software, Inkscape is a freely available software that performs essentially the same functions. All image manipulations are listed in detail below:

- In Figure 1 the images "Figure 1A_original.jpg" and "Figure 1B_original.jpg" from the Zenodo repository were merged, labeled, and annotated in one Figure using Inkscape.

- In Figure 3 three single frames of the video "Non-Woven_Detachement_from_Collector.mkv" in the Zenodo repository were captured using the VLC media player (v. 3.0.20, VideoLan Organization, Paris, France), merged into one figure, labeled, and annotated using Inkscape.

- In Figure 4 the images "Figure 4A_original.tif", "Figure 4B_original.tif", "Figure 4C_original.tif", and "Figure 4D_original.tif" from the Zenodo repository were merged, cropped, labeled, brightness and contrast optimized, and annotated in one Figure using Inkscape.

- In Figure 6 the images "Figure 6A_original.tif", "Figure 6B_original.tif", "Figure 6C_original.tif", and "Figure 6D_original.tif" from the Zenodo repository were merged, labeled, rotated, brightness and contrast optimized, and annotated in one Figure using Inkscape.

- In Figure 7 the images "Figure 7A_original.tif", "Figure 7B_original.tif", "Figure 7C_original.tif", and "Figure 7D_original.tif" from the Zenodo repository were merged, cropped, labeled, rotated, brightness and contrast optimized, and annotated in one Figure using Inkscape.

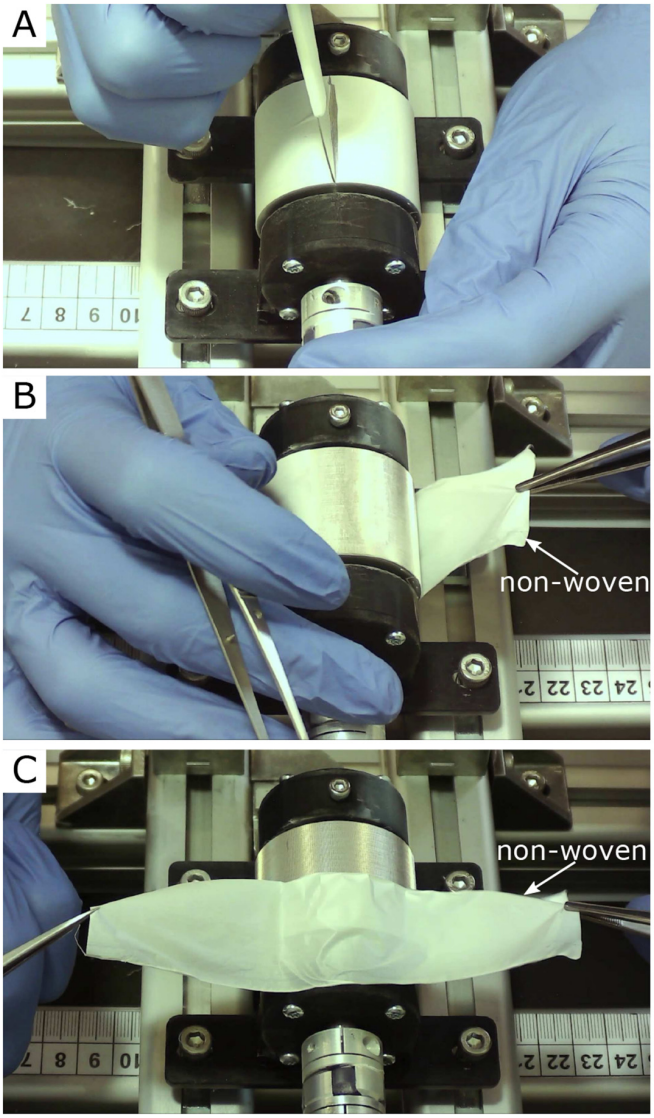

Figure 3. Removal process of the oriented nanofiber non-woven. (**A**) Cut open the fleece with a scalpel. (**B**) Remove the fleece with tweezers. (**C**) Fleece completely detached from the collector without leaving any residue on the collector.

- In the Figure S1 embedded in the underlaying data "Spatial period calculation.docx" the image "Figure S1A_original.tif" from the Zenodo repository was labeled and annotated using Corel Vector.
- In Figure S3 the images "Figure S3A_original.tif", "Figure S3B_original.tif", and "Figure S3C_original.tif" from the Zenodo repository were merged, cropped, labeled, brightness and contrast optimized, and annotated in one Figure using Inkscape.

Results

Aligned nanofibers

Figure 3A to C show an example of the detachment process for the nanofiber non-woven. It can be seen that the non-woven can be removed easily and without leaving any residue on the collector. The video "Non-Woven_Detachement_from_Collector.mkv" in the Zenodo repository (Lifka *et al.*, 2024) shows the removal process again in detail.

Figure 4 shows the SEM images of four different nanofiber non-woven samples. Figure 4A shows a non-woven with randomly oriented fibers (i.e. the collector did not rotate) as a control. Figure 4B to C show non-woven with increasing collector rotation speed. It can be clearly seen that the degree of orientation of the fibers increases with the rotational speed of the collector. While the orientation of the fibers still has potential for improvement at a rotational speed of v = 5 ms^{-1} (Figure 4B), a clear orientation in the horizontal direction can already be seen at a rotational speed of v = 8 ms^{-1} or v =14 ms^{-1} (Figure 4C and D).

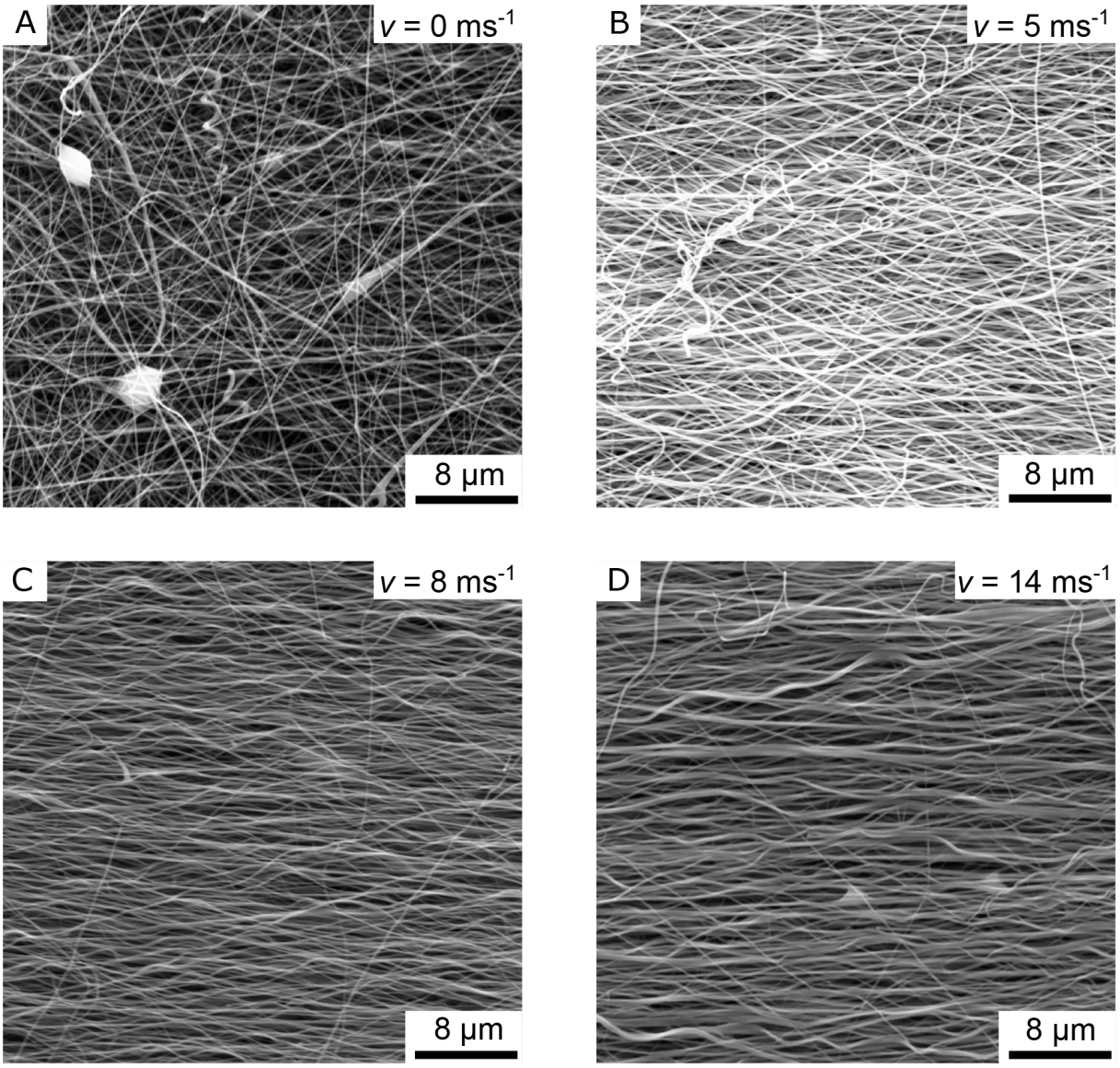

Figure 4. SEM images of the aligned nanofiber non-woven. (**A**) Randomly oriented nanofibers as control (i.e., the collector did not rotate, v = 0 ms^{-1}). (**B**) Nanofibers collected on the collector rotating with v = 5 ms^{-1}. (**C**) Nanofibers collected on the collector rotating with v = 8 ms^{-1}. (**D**) Nanofibers collected on the collector rotating with v = 14 ms^{-1}.

To better quantify the directionality of the fibers, Figure 5 shows the directionality histograms for all SEM images of Figure 4. A horizontal line in the images corresponds to an angle of 0° in the histogram. The dashed curve in red represents a normal distribution fit. It can be clearly seen that the sample with the randomly oriented fibers (Figure 5A) is relatively evenly distributed in all directions (standard deviation σ = 31.08°). The sample with v = 5 ms^{-1} (Figure 5B) is much more directional in comparison (σ = 19.68°). The samples in which the collector was rotated at v = 8 ms^{-1} (Figure 5C) and v = 14 ms^{-1} (Figure 5D) both exhibit excellent directionality (σ = 8.37° for 8 ms^{-1} and σ = 7.24° for 14 ms^{-1}).

Table 1 lists the average fiber diameters of the individual samples. On average across all samples, the fibers produced had a diameter of approx. 250 nm with a standard deviation of approximately 110 nm.

To investigate the directional cell growth on the samples, murine Schwann cells were cultured on an 8 ms^{-1} non-woven nanofiber sample (Figure 4C), which has a parallel fiber direction (Figure 5C) and on a sample with randomly oriented nanofibers as control. Despite the slightly smaller standard deviation of the 14 ms^{-1} (σ = 7.24°) sample in comparison to the 8 ms^{-1} (σ = 8.37°) sample, the 8 ms^{-1} was

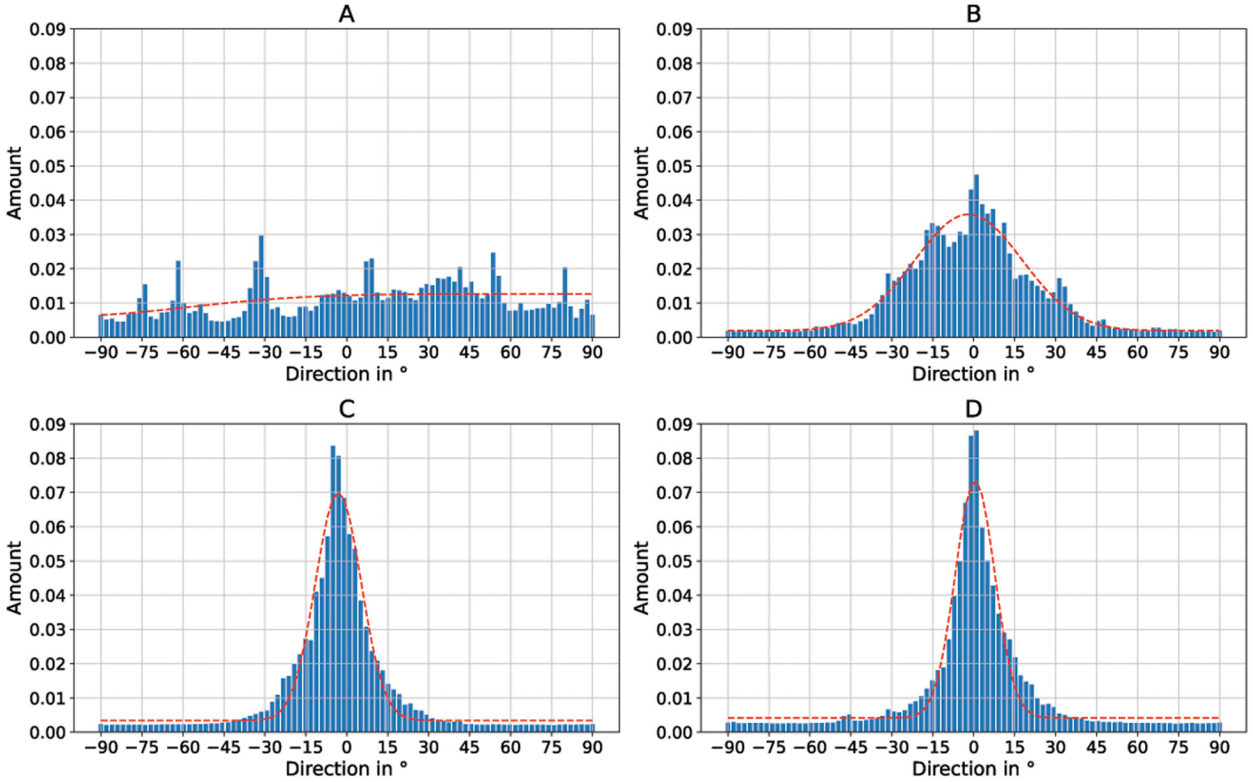

Figure 5. Directionality histograms of the non-woven. (**A**) Randomly oriented nanofibers as control (i.e., the collector did not rotate, v = 0 ms^{-1}) , σ = 31.08°). (**B**) Nanofibers collected on the collector rotating with v = 5 ms^{-1} (σ = 19.68°). (**C**) Nanofibers collected on the collector rotating with v = 8 ms^{-1} (σ = 8.37°). (**D**) Nanofibers collected on the collector rotating with v = 14 ms^{-1} (σ = 7.24°). The dashed red line represents a normal distribution fit of the histogram.

Table 1. Mean fiber diameters of the samples.

	Mean fiber diameter in nm	Standard deviation in nm
Randomly oriented	277.5	110.4
5 ms^{-1}	205.9	81.3
8 ms^{-1}	226.5	101.4
14 ms^{-1}	309.0	151.5
Overall	254.725	111.15

preferred. This is due to the fact that a rotational speed of 14 ms^{-1} pushes the limits of our setup and therefore the 8 ms^{-1} sample is much easier to produce and that the standard deviations of the two samples are de facto identical. The results can be seen in Figure 6A (randomly oriented) and C (aligned). A clear orientation of the cell growth in a horizontal direction can be seen in Figure 6C. Figure 6B and D show an enlarged section of Figure 6A and C, in which the non-woven under the cells is also visible. Note that the orientation of the nanofibers is also horizontal (i.e., parallel to the direction of cell growth) in Figure 6D. Similar to Figure 5, the directionality of the cell growth was quantified using Fourier analysis. The respective directionality histograms for the cells on nanofibers are shown in Figure 8A (randomly oriented) and Figure 8B (aligned). The directionality is based on the long axis of the cells, in other words the long axis of the cells corresponds to 0° in the histogram. Additionally, the fibers under the cells were also analyzed using Fourier analysis. The respective directionality histograms are shown in Figure S2 as underlying data in the Zenodo repository (Lifka *et al.*, 2024). The directional cell growth was investigated on n = 7 aligned 8 ms^{-1} nanofiber samples in total. All samples showed directional growth of the Schwann cells in fiber direction as presented in Figure 6. Therefore, Figure 6 shows a typical result of one specific sample.

In addition to the SEM images, Figure S3 in the Zenodo repository (Lifka *et al.*, 2024) shows fluorescence microscopy images of the cells on the non-woven. Figure S3A shows randomly oriented cells on a flat cover glass as control, Figure S3B shows randomly oriented cells on randomly oriented nanofibers, and Figure S3C shows oriented cells on aligned nanofibers. A brief description of the staining method used can be found in the file "Description_Staining_Method.docx" in the Zenodo repository (Lifka *et al.*, 2024).

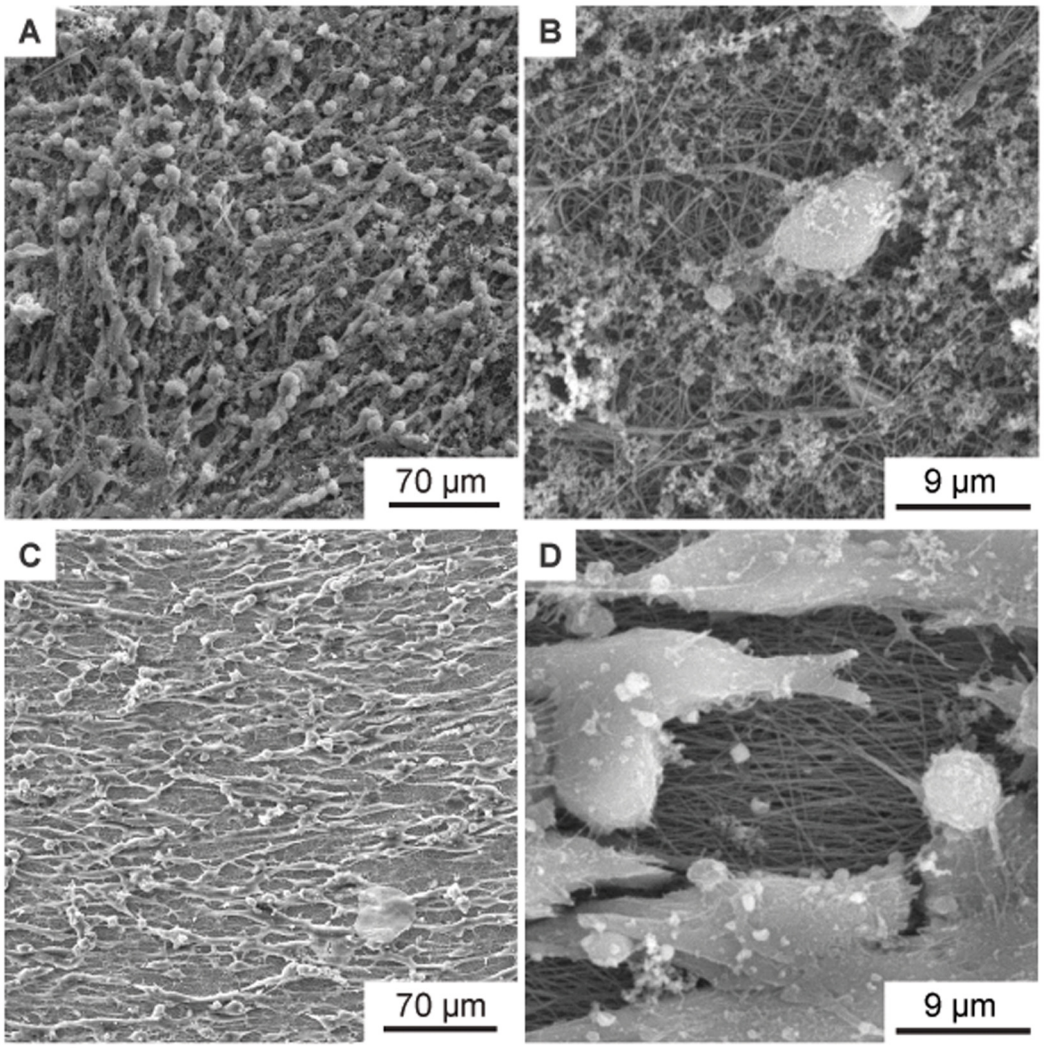

Figure 6. SEM images of murine Schwann cells cultivated for one week on electrospun PA-6 nanofibers. (**A**) Cells on randomly oriented nanofibers showing no orientation as control. (**B**) Magnified detail of (**A**) showing the randomly oriented nanofibers under the cells. (**C**) Cells with preferential orientation on aligned nanofibers (collector speed 8 ms-1). (**D**) Magnified detail of (**C**) showing the aligned nanofibers under the cells.

Nanoripples

Nanoripples (LIPSS) are structures that form upon laser irradiation on many materials, and originate from the interference of the incoming linearly polarized light of (ultra-)short pulsed lasers with the radiation remnants or plasmon modes in the surface (Bonse *et al.*, 2017). The orientation of the LIPSS can be either parallel or perpendicular to the polarization of the laser beam and their periodicity is comparable to the wavelength or smaller, depending on the laser fluence and the angle of incidence of the laser beam onto the irradiated substrate. In our case, the spatial period Λ of nanoripples fabricated using s-polarized laser light is given by $\Lambda = \lambda/(n_{eff} - \sin\theta)$, where λ is the wavelength of the laser beam, n_{eff} – the effective refractive index which lies between the refractive indices of air and PET (Barb *et al.*, 2014), and θ – the angle of incidence.

Figure 7A shows the murine Schwann cells cultivated for one week (same procedure as described above) on flat PET foil, used as reference sample. The cells show a random orientation and omnidirectional growth. In contrast, Figure 7B, showing murine Schwann cells cultivated for one week on PET nanoripples, proves the influence of nanorippled topography as external stimuli that renders cell alignment. Schwann cells exhibit a typical elongated bipolar shape and even though their sizes (in the order of some tens of micrometers) are much bigger than the nanoripples' height (above 110 nm (Buchberger *et al.*, 2023)) and periodicity (Λ = 331 ± 11 nm, N =10), the cells align and orient themselves along the LIPSS orientation. This effect happens due to the interaction of cell filopodia with the nano topography, as shown in Figure 7C. Figure 7D additionally shows the nanoripples without cells for better visibility. Again, the directionality

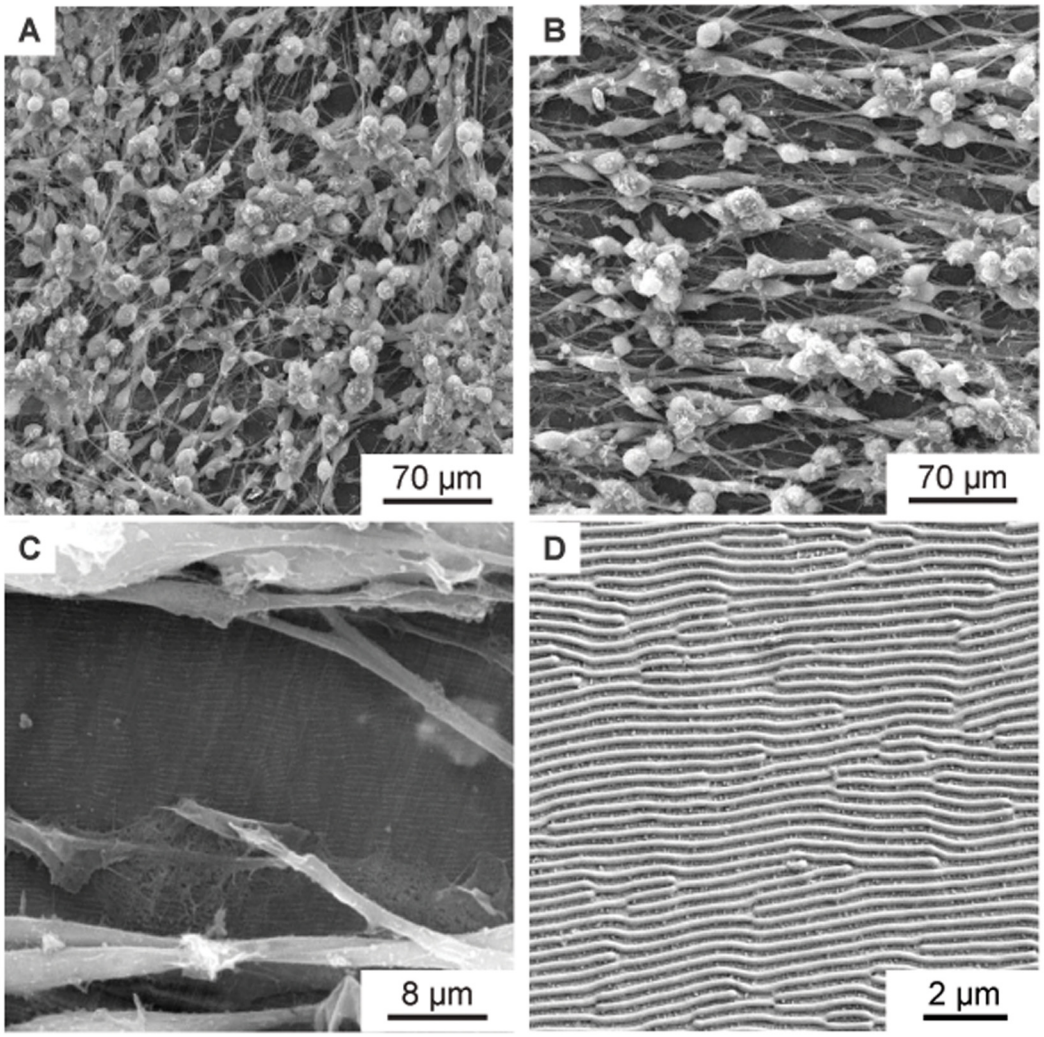

Figure 7. SEM images of aligned murine Schwann cells cultivated for one week on PET foils. (**A**) SEM image of murine Schwann cells cultivated for one week on flat PET foil, as control, showing no alignment. (**B**–**C**) SEM images of aligned murine Schwann cells cultivated for one week on a PET foil with nanoripples. (**C**) is a magnification of (**B**), showing an area with incomplete cell coverage, proving that the cells and the nanoripples have the same orientation. (**D**) SEM image showing the nanoripples without cells.

histograms of the directed cell growth are shown in Figure 8C for the flat PET foil sample and in Figure 8D for the PET foil sample with nanoripples. Again, the long axis of the cells corresponds to 0° in the histogram.

Discussion

In this work, two methods are described to present an improved directed growth of Schwann cells, a type of glial cell that insulates and protects the axons of neurons. Major injuries of nerve tissue are often characterized by poor functional regeneration and therefore require conduits that promote healing of the nerve axons and provide direction for Schwann cell growth. One method uses laser-induced periodic surface structures (LIPSS) that mimic the nanofeatures found in the extracellular matrix. These LIPSS can be used to specify the direction of growth for Schwann cells and promote growth in a specific direction. As we have reported before (Barb *et al.*, 2014; Barb *et al.*, 2015; Rebollar *et al.*, 2008), different types of mammalian cells can be aligned by parallel quasi-periodic grooves or ripples on the underlying substrate even though the lateral dimensions of the cells are much larger than the structures as well as the height of the cells is much larger than the structure height. The lateral periodicities of the ripples or groove reach from a few hundred nm to a few µm with structure heights of a few ten to a few hundred nm, respectively. In this regime, which could be addressed as "surface-induced alignment", the alignment of cells is based on organization of the fibrils of the cell cytoskeleton especially in protrusions of the cells (Peterbauer *et al.*, 2010). For larger structure periodicities and structure heights, as for instance in (Babaliari *et al.*, 2021), the structure dimensions become comparable to those of the cells and we see a "contact guidance" of the whole

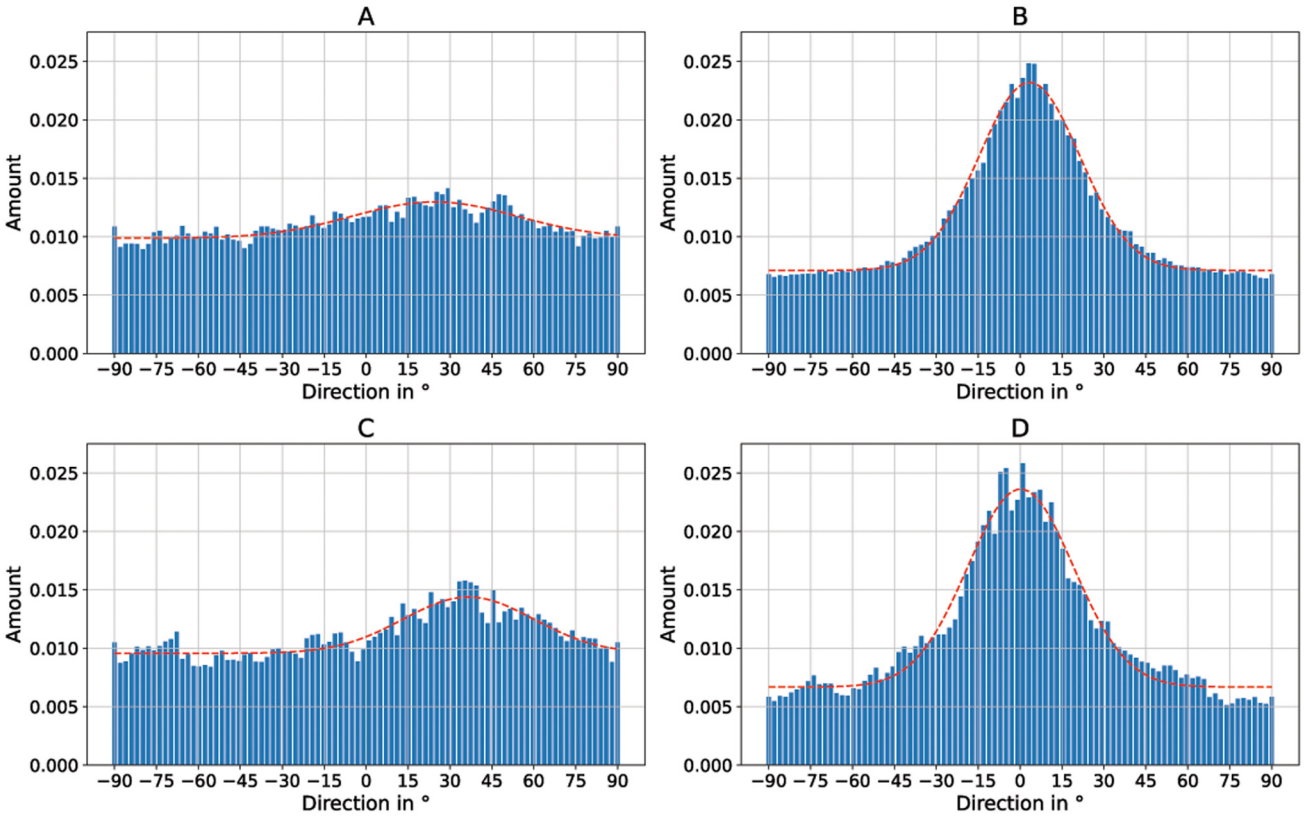

Figure 8. Directionality histograms of the murine Schwann cells cultivated on electrospun PA-6 nanofibers and PET foils. (**A**) Cells on randomly oriented nanofibers (σ = 29.51°). (**B**) Cells on aligned nanofibers (σ = 18.06°). (**C**) Cells on flat PET foil (σ = 23.37°). (**D**) Cells on PET foil with nanoripples. (σ = 18.95°). The dashed red line represents a normal distribution fit of the histogram.

cells by the structure walls. When the oriented topographic features on a surface are too small, the cells cannot align along these structures any more. For laser-induced ripples, cell alignment is observed only when the periodicity is above a critical periodicity threshold (about 300 nm), which is cell type specific (Rebollar *et al.*, 2008). For surface-induced alignment, we saw no qualitative difference in cell alignment depending on the structure size, at least not for human myoblasts (see (Barb *et al.*, 2014; Barb *et al.*, 2015)). Both methods presented here provide parallel features which correspond to surface-induced alignment regime and we show here for the first time that they can be used for the orientation of Schwann cells, in deed. However, we expect no strong qualitative effect of a variation of the structure size (within this regime) on the alignment.

This is, however, limited to more or less rigid (in this case) PET films. Laser-induced nanoripples were reported on a number of other polymers, for instance polystyrene (PS) (Rebollar *et al.*, 2008), poly (trimethylene terephthalate) and poly (carbonate bisphenol A) (Rebollar *et al.*, 2012), poly(carbonate) (PC) (Csete *et al.*, 2001; Mezera *et al.*, 2019), the epoxy resin SU-8 (Plamadeala *et al.*, 2023), conjugated polymers (Rodríguez-Rodríguez *et al.*, 2018), or poly(imide) (PI) (Baudach *et al.*, 1999). These polymers have different material properties to PET to a certain extent, but are all fairly inflexible as they are several 10 µm thick sheets, rigid plates, or thin films on rigid substrates. They are therefore only suitable to a limited extent as nerve-conducting fillers in a flexible nerve regeneration conduit, but may be used as a hollow tube connecting two nerve ends in cases where extremely high flexibility is not absolutely necessary. There are a few approaches to produce laser-induced nanoripples on very thin flexible polymer films (Buchberger *et al.*, 2024) or on bendable polymer microfibers (Sajzew *et al.*, 2015), but these materials are very delicate to handle.

Therefore, an alternative method describes the production of a non-woven consisting of parallel, aligned nanofibers. This non-woven is extremely flexible and can be adapted to many different shapes. The method is based on the electrospinning process and uses a very fast rotating cylindrical collector to produce directed nanofibers. The unique feature of this method in comparison to existing techniques is the special surface structure (Lifka *et al.*, 2023) of the collector, which enables the non-woven to be easily removed without additional coating and additional effort. (i.e., a supportless electrospinning process).

These extremely flexible non-woven nanofiber mats have huge potential for use in the manufacturing of 3D-conduits for nerve regeneration. The nanofiber sheets can easily be rolled up in the axial direction of the fibers. This results in a thin roll of nanofiber non-woven with the nanofiber orientation in axial direction. One or more of these rolls could now be used as a conduit for nerve regeneration by connecting the two ends of a damaged nerve pathway and thus simply bridging large defects. The aligned nanofibers now act as an orientation aid for the nerve cells, which can thus repair the defects more easily and quickly. Additionally, a thin laser-structured polymer foil can be wrapped around the nanofiber conduit in order to increase the stability of the whole conduit, which would combine the two presented methods in one application.

In the results presented here, the samples were coated with PLL to improve cell adhesion to the nanofibers. We observed that although the cells adhere without PLL coating, they immediately detach from the fibers at the slightest mechanical stress. For this reason, all experiments presented here were carried out with PLL-coated samples. For the sake of completeness, Figure S4 shows an SEM image of aligned Schwann cells on aligned nanofibers that were not PLL coated. Visually, there is no significant difference to PLL coated samples.

As shown in Table 1, the mean fiber diameter increases with the rotational speed. From Figure 5, it seems that the fiber shape changes to a more ribbon-like shape with increasing rotational speed, which may explain the increasing measured mean diameter. However, this phenomenon was not further investigated in the course of this work and is thus the subject of future research.

In this work, only one fiber material was tested, namely PA-6, as good experience has already been made with this polymer. Of course, this method can also be applied to biocompatible polymers, such as fibers made of cellulose acetate butyrate (CAB) or collagen fibers. These materials would be very well suited for use in nerve regeneration. The method presented here can easily be adapted for these materials. Only the relevant parameters, such as the rotational speed of the collector and the volume flow of the electrospinning solution, need to be determined and adapted accordingly.

Conclusion

In this paper we show that oriented mechanical nanofeatures, such as electrospun aligned nanofibers and nanoripples produced by means of LIPSS on PET foils, are able to mimic the extracellular matrix features, and stimulate the elongation and support the alignment of Schwann cells. In particular, conduits made of flexible, rolled-up oriented nanofibers and hollow tubes of thin polymer foils with nanoripples could lead to better axonal regeneration in patients with severe nerve track injuries.

Ethics and consent

Ethical approval and consent were not required.

Data and software availability

Underlying data

Zenodo: Repository for the Method Article "Oriented artificial nanofibers and laser induced periodic surface structures as substrates for Schwann cells alignment". https://doi.org/10.5281/zenodo.13944609 (Lifka *et al.*, 2024).

This project contains the following underlying data:

- Directionality_Hist.py. (Python file for generating directionality histograms of the non-woven.)
- RandomHist.csv. (Histogram data from ImageJ for randomly oriented non-woven.)
- 5mpsHist.csv. (Histogram data from ImageJ for 5 ms^{-1} non-woven.)
- 8mpsHist.csv. (Histogram data from ImageJ for 8 ms^{-1} non-woven.)
- 14mpsHist.csv. (Histogram data from ImageJ for 14 ms^{-1} non-woven.)
- RandFibersHist.csv (Histogram data from ImageJ for cells on randomly oriented non-woven.)
- Fibers8mpsHist.csv (Histogram data from ImageJ for cells on 8 ms -1 non-woven.)
- RandFoilHist.csv (Histogram data from ImageJ for flat PET foil.)
- DirFoilHist.csv (Histogram data from ImageJ for PET foils with ripples.)
- RandFibersUnderCellsHist.csv (Histogram data from ImageJ for randomly oriented non-woven under the cells from Figure 6B.)
- Fibers8mps_FibersUnderCellsHist.csv (Histogram data from ImageJ for 8 ms -1 non-woven under the cells from Figure 6D.)
- DiameterAnalysisRandom.csv. (Fiber diameter analysis and histogram data from ImageJ for random oriented non-woven.)
- DiameterAnalysis5mps.csv. (Fiber diameter analysis and histogram data from ImageJ for 5 ms^{-1} non-woven.)
- DiameterAnalysis8mps.csv. (Fiber diameter analysis and histogram data from ImageJ for 8 ms^{-1} non-woven.)
- DiameterAnalysis14mps.csv. (Fiber diameter analysis and histogram data from ImageJ for 14 ms^{-1} non-woven.)

- Spatial period calculation.docx. (Word file containing the data for the spatial period calculation of the nanoripples.)
- Description_Staining_Method.docx. (Word file containing a brief description of the staining method used for fluorescence microscopy.)
- Figure 1A_original.jpg. (Original unmanipulated image used for Figure 1A.)
- Figure 1B_original.jpg. (Original unmanipulated image used for Figure 1B.)
- Figure 4A_original.tif. (Original unmanipulated image used for Figure 4A.)
- Figure 4B_original.tif. (Original unmanipulated image used for Figure 4B.)
- Figure 4C_original.tif. (Original unmanipulated image used for Figure 4C.)
- Figure 4D_original.tif. (Original unmanipulated image used for Figure 4D.)
- Figure 6A_original.tif. (Original unmanipulated image used for Figure 6A.)
- Figure 6B_original.tif. (Original unmanipulated image used for Figure 6B.)
- Figure 6C_original.tif. (Original unmanipulated image used for Figure 6C.)
- Figure 6D_original.tif. (Original unmanipulated image used for Figure 6D.)
- Figure 7A_original.tif. (Original unmanipulated image used for Figure 7A.)
- Figure 7B_original.tif. (Original unmanipulated image used for Figure 7B.)
- Figure 7C_original.tif. (Original unmanipulated image used for Figure 7C.)
- Figure 7D_original.tif. (Original unmanipulated image used for Figure 7D and Figure S1A.)
- Figure S1A_original.tif. (Original unmanipulated image used for Figure S1A.)
- Figure S2.png. (Directionality histograms of the fibers under the cells from Figure 6B and D)
- Figure S3.png. (Fluorescence microscopy image of Schwann cells.)
- Figure S3A_original.tif. (Original unmanipulated image of Figure S3A.)
- Figure S3B_original.tif. (Original unmanipulated image of Figure S3B.)
- Figure S3C_original.tif. (Original unmanipulated image of Figure S3C.)
- Figure S4.tif. (Original unmanipulated SEM image of aligned Schwann cells on aligned nanofibers without PLL coating.)

Extended data

Zenodo: Repository for the Method Article "Oriented artificial nanofibers and laser induced periodic surface structures as substrates for Schwann cells alignment". https://doi.org/10.5281/zenodo.13944609 (Lifka *et al.*, 2024).

This project contains the following extended data:

- Bearing bracket Fixed bearing.step. (CAD .step file for the fixed bearing bracket of the rotating drum collector setup.)
- Bearing bracket loose fit bearing.step. (CAD .step file for the loose bearing bracket of the rotating drum collector setup.)
- Bearing cover Fixed bearing.step. (CAD .step file for the fixed bearing cover of the rotating drum collector setup.)
- Bearing cover loose fit bearing.step. (CAD .step file for the loose bearing cover of the rotating drum collector setup.)
- Motor mount.step. (CAD .step file for the DC motor mount of the rotating drum collector setup.)
- Surface structured collector.step. (CAD .step file for the surface-structured rotating drum collector.)
- Surface Structured Collector Drawing.pdf. (2D drawing of the rotating drum collector.)
- Setup Rotating Collector.pdf. (2D drawing of the whole rotating drum collector setup.)
- Non-Woven_Detachement_from_Collector.mkv (Short video showing the detachment process of the non-woven fabric from the surface-structured collector.)

Data are available under the terms of the Creative Commons Attribution 4.0 International (CC-BY 4.0).

Acknowledgements

We would like to thank ZONA for their support and assistance in the production of the surface-structured collector for the electrospinning process.

References

Babaliari E, Kavatzikidou P, Mitraki A, *et al.*: **Combined effect of shear stress and laser-patterned topography on Schwann cell outgrowth: synergistic or antagonistic?** *Biomater Sci.* 2021; **9**(4): 1334–1344.
PubMed Abstract | **Publisher Full Text**

Barb RA, Hrelescu C, Dong L, *et al.*: **Laser-induced periodic surface structures on polymers for formation of gold nanowires and activation of human cells.** *Appl Phys A.* 2014; **117**(1): 295–300.
Publisher Full Text

Barb RA, Magnus B, Innerbichler S, *et al.*: **VUV treatment combined with mechanical strain of stretchable polymer foils resulting in cell alignment.** *Appl Surf Sci.* 2015; **325**(C): 105–111.
Publisher Full Text

Baudach S, Bonse J, Kautek W: **Ablation experiments on polyimide with femtosecond laser pulses.** *Appl Phys A: Mater Sci Process.* 1999; **69**(7): S395–S398.
Publisher Full Text

Bonse J, Höhm S, Kirner SV, *et al.*: **Laser-induced periodic surface structures— a scientific evergreen.** *IEEE J Sel Top Quantum Electron.* 2017; **23**(3): 9000615, 109–123.
Publisher Full Text

Buchberger G, Kührer M, Hesser G, *et al.*: **Nanoscale dots, grids, ripples, and hierarchical structures on PET by UV laser processing.** *Photonics.* 2024; **11**(2): 184.
Publisher Full Text

Buchberger G, Meyer M, Plamadeala C, *et al.*: **Robustness of antiadhesion between nanofibers and surfaces covered with nanoripples of varying spatial period.** *Front Ecol Evol.* 2023; **11**: fevo.2023.1149051.
PubMed Abstract | **Publisher Full Text** | **Free Full Text**

Cattin AL, Burden JJ, Van Emmenis L, *et al.*: **Macrophage-induced blood vessels guide Schwann cell-mediated regeneration of peripheral nerves.** *Cell.* 2015; **162**(5): 1127–1139.
PubMed Abstract | **Free Full Text**

Chen Y, Zhao W, Dai H: **Porous PLGA-PEG nerve conduit decorated with oriented electrospun chitosan-RGD nanofibre.** *J Mater Res Technol.* 2021; **15**: 86–98.
Publisher Full Text

Csete M, Marti O, Bor ZS: **Laser-Induced Periodic Surface Structures on different poly-carbonate films.** *Applied Physics A.* 2001; **73**(4): 521–526.
Publisher Full Text

Fosodeder P, Baumgartner W, Steinwender C, *et al.*: **Repellent rings at titanium cylinders against overgrowth by fibroblasts.** *Adv Opt Technol.* 2020; **9**(3): 113–120.
Publisher Full Text

Heitz J, Buchberger G, Baumgartner W, *et al.*: **Change of adhesion properties of bioinspired laser-induced periodic nanostructures towards cribellate spider nanofiber threads by means of thin coatings.** *Coatings.* 2024; **14**(7): 790.
Publisher Full Text

Hotaling NA, Bharti K, Kriel H, *et al.*: **DiameterJ: a validated open source nanofiber diameter measurement tool.** *Biomaterials.* 2015; **61**: 327–338.
PubMed Abstract | **Publisher Full Text** | **Free Full Text**

Huang C, Ouyang Y, Niu H, *et al.*: **Nerve guidance conduits from aligned nanofibers: improvement of nerve regeneration through longitudinal nanogrooves on a fiber surface.** *ACS Appl Mater Interfaces.* 2015; **7**(13): 7189–7196.
PubMed Abstract | **Publisher Full Text**

Hunter JD: **Matplotlib: a 2D graphics environment.** *Comput Sci Eng.* 2007; **9**(3): 90–95.
Publisher Full Text

Jessen KR, Mirsky R: **The success and failure of the Schwann cell response to nerve injury.** *Front Cell Neurosci.* 2019; **13**: 33,1–14.
PubMed Abstract | **Publisher Full Text** | **Free Full Text**

Jiang M, Chen M, Liu N: **Interactions between Schwann cell and extracellular matrix in peripheral nerve regeneration.** *Front Neurol.* 2024; **15**: 1372168.
PubMed Abstract | **Publisher Full Text** | **Free Full Text**

Kriebel A, Hodde D, Kuenzel T, *et al.*: **Cell-free artificial implants of electrospun fibres in a three-dimensional gelatin matrix support sciatic nerve regeneration *in vivo*.** *J Tissue Eng Regen Med.* 2017; **11**(12): 3289–3304.
PubMed Abstract | **Publisher Full Text**

Lifka S, Plamadeala C, Weth A, *et al.*: **Repository for the method article "oriented artificial nanofibers and laser induced periodic surface structures as substrates for Schwann cells alignment"**. *Zenodo.* 2024.
http://www.doi.org/10.5281/zenodo.13944609

Lifka S, Stecher C, Meyer M, *et al.*: **Biomimetic, antiadhesive surface structure inspired by the calamistra setae of cribellate spiders for electrospun nanofiber handling.** *Front Ecol Evol.* 2023; **11**: 1099355.
Publisher Full Text

Maalouf M, Abou Khalil A, Di Maio Y, *et al.*: **Polarization of Femtosecond Laser for titanium alloy nanopatterning influences osteoblastic differentiation.** *Nanomaterials (Basel).* 2022; **12**(10): 1619.
PubMed Abstract | **Publisher Full Text** | **Free Full Text**

Manganas P, Kavatzikidou P, Kordas A, *et al.*: **The role of mechanobiology on the Schwann cell response: a tissue engineering perspective.** *Front Cell Neurosci.* 2022; **16**: 948454.
PubMed Abstract | **Free Full Text**

Meena P, Kakkar A, Kumar M, *et al.*: **Advances and clinical challenges for translating nerve conduit technology from bench to bed side for peripheral nerve repair.** *Cell Tissue Res.* 2021; **383**(2): 617–644.
PubMed Abstract | **Publisher Full Text**

Mezera M, Bonse J, Römer G: **Influence of bulk temperature on laser-induced periodic surface structures on polycarbonate.** *Polymers (Basel).* 2019; **11**(12): 1947.
PubMed Abstract | **Publisher Full Text** | **Free Full Text**

Millesi F, Weiss T, Mann A, *et al.*: **Defining the regenerative effects of native spider silk fibers on primary Schwann cells, sensory neurons, and nerve-associated fibroblasts.** *FASEB J.* 2021; **35**(2): e21196.
PubMed Abstract | **Publisher Full Text** | **Free Full Text**

Muck M, Wolfsjäger B, Seibert K, *et al.*: **Femtosecond laser-processing of pre-anodized Ti-based bone implants for cell-repellent functionalization.** *Nanomaterials (Basel).* 2021; **11**(5): 1342.
PubMed Abstract | **Publisher Full Text** | **Free Full Text**

Peterbauer T, Yakunin S, Siegel J, *et al.*: **Dynamics of the alignment of mammalian cells on a nano-structured polymer surface.** *Macromol Symp.* 2010; **296**(1): 272–277.
Publisher Full Text

Plamadeala C, Lifka S, Buchberger G, *et al.*: **Bio-inspired hierarchical polymer micro- and nanostructures for anti-adhesion applications.** *Front Mater.* 2023; **10**: 1281992.
Publisher Full Text

Rebollar E, Frischauf I, Olbrich M, *et al.*: **Proliferation of aligned mammalian cells on laser-nanostructured polystyrene.** *Biomaterials.* 2008; **29**(12): 1796–1806.
PubMed Abstract | **Publisher Full Text**

Rebollar E, Vázquez De Aldana JR, Pérez-Hernández JA, *et al.*: **Ultraviolet and infrared femtosecond laser induced periodic surface structures on thin polymer films.** *Appl Phys Lett.* 2012; **100**(4): 041106.
Publisher Full Text

Richter AM, Buchberger G, Stifter D, *et al.*: **Spatial period of laser-induced surface nanoripples on PET determines *Escherichia coli* repellence.** *Nanomaterials (Basel).* 2021; **11**(11): 3000.
PubMed Abstract | **Publisher Full Text** | **Free Full Text**

Rodríguez-Rodríguez Á, Rebollar E, Ezquerra TA, *et al.*: **Patterning conjugated polymers by laser: synergy of nanostructure formation in the all-polymer heterojunction P3HT/PCDTBT.** *Langmuir.* 2018; **34**(1): 115–125.
PubMed Abstract | **Publisher Full Text**

Sajzew R, Schröder J, Kunz C, *et al.*: **Femtosecond laser-induced surface structures on carbon fibers.** *Opt Lett.* 2015; **40**(24): 5734–7.
PubMed Abstract | **Publisher Full Text**

Schnell E, Klinkhammer K, Balzer S, *et al.*: **Guidance of glial cell migration and axonal growth on electrospun nanofibers of poly-ε-caprolactone and a collagen/poly-ε-caprolactone blend.** *Biomaterials.* 2007; **28**(19): 3012–3025.
PubMed Abstract | **Publisher Full Text**

Stadlmayr S, Peter K, Millesi F, *et al.*: **Comparative analysis of various spider silks in regard to nerve regeneration: material properties and Schwann cell response.** *Adv Healthc Mater.* 2024; **13**(8): e2302968.
PubMed Abstract | **Publisher Full Text** | **Free Full Text**

Wang J, Tian L, Chen N, *et al.*: **The cellular response of nerve cells on poly-l-lysine coated PLGA-MWCNTs aligned nanofibers under electrical stimulation.** *Mater Sci Eng C Mater Biol Appl.* 2018; **91**: 715–726.
PubMed Abstract | **Publisher Full Text**

Wang J, Xiong H, Zhu T, *et al.*: **Bioinspired multichannel nerve guidance conduit based on shape memory nanofibers for potential application in peripheral nerve repair.** *ACS Nano.* 2020; **14**(10): 12579–12595.
PubMed Abstract | **Publisher Full Text**

Yiannakou C, Simitzi C, Manousaki A, *et al.*: **Cell patterning via laser micro/nano structured silicon surfaces.** *Biofabrication.* 2017; **9**(2): 025024.
PubMed Abstract | **Publisher Full Text**

Open Peer Review

Current Peer Review Status: ✔ ? ✔

Version 3

Reviewer Report 06 November 2024

https://doi.org/10.21956/openreseurope.20321.r45362

© **2024 Chu T.** This is an open access peer review report distributed under the terms of the Creative Commons Attribution License, which permits unrestricted use, distribution, and reproduction in any medium, provided the original work is properly cited.

✔ **Tak-Ho Chu**
University of Calgary, Calgary, Canada

I reviewed the article carefully, and the authors have satisfactorily addressed all my concerns. I am pleased to approve the manuscript; however, I suggest that the authors revise the discussion for greater coherence.

Competing Interests: No competing interests were disclosed.

Reviewer Expertise: Peripheral nerve injury and repair, Schwann cell biology

I confirm that I have read this submission and believe that I have an appropriate level of expertise to confirm that it is of an acceptable scientific standard.

Version 2

Reviewer Report 19 September 2024

https://doi.org/10.21956/openreseurope.19906.r44238

© **2024 Chu T.** This is an open access peer review report distributed under the terms of the Creative Commons Attribution License, which permits unrestricted use, distribution, and reproduction in any medium, provided the original work is properly cited.

✘ **Tak-Ho Chu**
University of Calgary, Calgary, Canada

The manuscript by Lifka et al. investigates an improved method for generating aligned electro spun fibres and laser-induced nanoripples on PET foils to promote Schwann cell alignment in

nerve guide materials. The authors employed scanning electron microscopy to examine an immortalized mouse Schwann cell line on these materials and concluded that both methods allow Schwann cells to align parallel to the direction of the fibers and nanoripples.
While the manuscript provides sufficient evidence of Schwann cell alignment, several methodologies are lacking that are crucial for fully evaluating the study. My major concern is that the authors state in the Discussion that nanoripple formation on stiff materials limits its application (if I understand correctly), which is why electro spun fibres were investigated. Firstly, the order of these two experiments is reversed in the Results section. Secondly, it is neither shown nor discussed whether laser-induced nanoripples can form on softer materials. Therefore, the rationale behind the experiments needs further clarification and should be explicitly stated in the Introduction. Additionally, a brief literature review should be provided to outline the current development of nerve guides, their associated challenges, and what the authors aim to advance in the field.
The manuscript would be significantly improved if the authors could address the following points:

1. Is PLL coating required for cell attachment to the electro spun fibres? If not, an experiment without PLL coating should be included. The authors should also discuss the materials used: are they biocompatible? Do they trigger an inflammatory response? Are they biodegradable? If the focus is solely on the technique rather than the materials, please discuss how easily these techniques can be applied to appropriate materials in the future.
2. References on nerve regeneration are missing. Readers unfamiliar with this field may benefit from the following reviews: Jessen and Mirsky, *The Success and Failure of the Schwann Cell Response to Nerve Injury*, *Front. Cell. Neurosci.*, 2019, and Cattin et al., *Macrophage-Induced Blood Vessels Guide Schwann Cell-Mediated Regeneration of Peripheral Nerves*, *Cell*, 2015. Additionally, please provide references supporting the statement in the Introduction that Schwann cell orientation depends on ECM or the supporting material. Schwann cells tend to align in a parallel fashion in culture when near confluence.
3. Regarding LIPSS, please clarify why the particular laser settings were chosen and why they are suitable for Schwann cells.
4. The authors should discuss how these techniques could be applied in a 3D configuration for nerve conduits.
5. The staining method should be described, perhaps in supplementary data.
6. How many samples were used for data analysis?
7. Why was 8 m/s chosen for further study in cell seeding? Fibers generated at 14 m/s appear to have a narrower peak, suggesting better alignment than those produced at 8 m/s. Can the authors provide a statistical comparison between these methods, perhaps through the area under the curve? Similarly, is there a statistical difference between fiber diameters at different speeds? The implications of fiber diameter and how it affects cell kinetics should be discussed.
8. How was the directionality of cells determined? Was it based on the long axis of the cells?

References

1. Jessen KR, Mirsky R: The Success and Failure of the Schwann Cell Response to Nerve Injury.*Front Cell Neurosci*. 2019; **13**: 33 PubMed Abstract | Publisher Full Text
2. Cattin AL, Burden JJ, Van Emmenis L, Mackenzie FE, et al.: Macrophage-Induced Blood Vessels Guide Schwann Cell-Mediated Regeneration of Peripheral Nerves.*Cell*. 2015; **162** (5): 1127-39 PubMed Abstract | Publisher Full Text

Is the rationale for developing the new method (or application) clearly explained?
Partly

Is the description of the method technically sound?
Partly

Are sufficient details provided to allow replication of the method development and its use by others?
Partly

If any results are presented, are all the source data underlying the results available to ensure full reproducibility?
Yes

Are the conclusions about the method and its performance adequately supported by the findings presented in the article?
Partly

Competing Interests: No competing interests were disclosed.

Reviewer Expertise: Peripheral nerve injury and repair, Schwann cell biology

I confirm that I have read this submission and believe that I have an appropriate level of expertise to state that I do not consider it to be of an acceptable scientific standard, for reasons outlined above.

Author Response 18 Oct 2024

Sebastian Lifka

First of all, we would like to thank the reviewer for the helpful comments and suggestions on our manuscript and it is with great pleasure that we upload a revised version. We can understand the concern of the reviewer. Therefore, we now explain that laser-induced nanoripples have also been observed in a number of other polymers. These polymers have different material properties to PET to a certain extent, but are all fairly inflexible as they are several 10 µm thick sheets, rigid plates or thin films on rigid substrates. They are therefore only suitable to a limited extent as nerve-conducting fillers in a flexible nerve regeneration conduit. There are a few approaches to produce laser-induced nanoripples on very thin flexible polymer films or on bendable polymer microfibers, but these materials are very delicate to handle. Therefore, an alternative method describes the production of a non-woven consisting of nanofibers. This non-woven is extremely flexible and can be adapted to many different shapes. It could be rolled up to fill a nerve regeneration conduit. These considerations (together with a number of new references) have been added partly to the Introduction and mainly to the Discussion section. Regarding the order of the experiments in the Results section. As the main focus is more on the nanofiber-method, this method is treated first in the Introduction, Materials, and Results section. In the Discussion, we start

with the LIPSS method and conclude with the nanofiber method, partly for reasons of argumentation and partly for didactic reasons, as we would like to end with the main focus. Furthermore, we complemented the introduction with a brief literature review about state-of-the-art nerve guides. Please find below our detailed responses to the comments.

Comment #1: Is PLL coating required for cell attachment to the electro spun fibres? If not, an experiment without PLL coating should be included. The authors should also discuss the materials used: are they biocompatible? Do they trigger an inflammatory response? Are they biodegradable? If the focus is solely on the technique rather than the materials, please discuss how easily these techniques can be applied to appropriate materials in the future.

Author response: *Thank you very much for this question. PLL coating is not absolutely necessary for cell attachment, but we observed that cell attachment is much better with PLL coating. If the fibers are not coated, the samples have to be treated very carefully, otherwise the cells tend to detach. Thus, to ease the handling of the samples, we decided to perform PLL coating for every sample. We discussed this also in the manuscript, and added a SEM image (Figure S4) showing Schwann cells on an uncoated sample as a supplement to the Zenodo repository. Regarding the materials used, the PA6 used here for the nanofibers is not biocompatible. We are currently working on implementing this method for biocompatible materials such as CAB. PA6 currently works best with the setup used. In this work, we were primarily concerned with the method and less with the materials themselves. We have added a statement to the manuscript in which we discuss the transfer of this method to biocompatible materials.*

Comment #2: References on nerve regeneration are missing. Readers unfamiliar with this field may benefit from the following reviews: Jessen and Mirsky, The Success and Failure of the Schwann Cell Response to Nerve Injury, Front. Cell. Neurosci., 2019, and Cattin et al., Macrophage-Induced Blood Vessels Guide Schwann Cell-Mediated Regeneration of Peripheral Nerves, Cell, 2015. Additionally, please provide references supporting the statement in the Introduction that Schwann cell orientation depends on ECM or the supporting material. Schwann cells tend to align in a parallel fashion in culture when near confluence.

Author response: *Thank you very much for providing us with these beneficial references, we added them in the introduction section. Furthermore, we provided references supporting the statement in the Introduction that Schwann cell orientation depends on ECM or the supporting material (Jiang et al., 2024; Manganas et al., 2022).*

Comment #3: Regarding LIPSS, please clarify why the particular laser settings were chosen and why they are suitable for Schwann cells.

Author response:*These parameters were investigated in previous works (Barb et al., 2014, Barb et al., 2015, and Peterbauer et al., 2010). In the parameter range where "surface-induced alignment" appears, no qualitative difference of the alignment effect could be observed. However, we expect no strong qualitative effect of a variation of the structure size (within this regime) on the alignment. We discussed this in the discussion section.*

Comment #4: The authors should discuss how these techniques could be applied in a 3D configuration for nerve conduits.

Author response: *As stated above, the LIPSS on PET-foils are rather inflexible and therefore are only suitable to a limited extent as nerve guiding fillers in a bendable nerve regeneration conduit, but may be used as a hollow tube connecting two nerve ends in cases where extremely high flexibility is not absolutely necessary. Thus, we describe an alternative method using flexible, aligned nanofibers. These very thin nanofiber sheets can easily be rolled up in the axial direction of the fibers. This results in a thin roll of nanofiber non-woven with the nanofiber orientation in axial direction. One or more of these rolls could now be used as a conduit for nerve regeneration. Additionally, a thin laser-structured polymer foil can be wrapped around the nanofiber conduit in order to increase the stability of the whole conduit. To make this point clear, we described this intended process in the manuscript.*

Comment #5: The staining method should be described, perhaps in supplementary data.

Author response: *As requested, we added a brief description of the staining method in the supplementary data.*

Comment #6: How many samples were used for data analysis?

Author response: *In total, n = 7 samples for cells on aligned nanofibers where investigated. The here presented data show the typical results of one specific sample. We clarified this in the manuscript. As the method with LIPSS on PET foils was basically already investigated and the functionality could be shown for other types of cells in previous works (Peterbauer, 2008), the sample size of the LIPSS was n = 1. Only one sample was examined here to verify that this method also works for Schwann cells. As can be seen from the manuscript, this was also confirmed.*

Comment #7: Why was 8 m/s chosen for further study in cell seeding? Fibers generated at 14 m/s appear to have a narrower peak, suggesting better alignment than those produced at 8 m/s. Can the authors provide a statistical comparison between these methods, perhaps through the area under the curve? Similarly, is there a statistical difference between fiber diameters at different speeds? The implications of fiber diameter and how it affects cell kinetics should be discussed.

Author response: *Thank you for this important question. From the directionality analysis of the 8 m/s and the 14 m/s sample, it can be concluded that the two samples are more or less equal in terms of directionality. To quantify this assertion, we added and discussed the respective σ values (i.e., the standard deviation) of the Gaussian-Fit-curves (dashed red line) in the histograms. The standard deviation of the 8 m/s sample is with 8° nearly identical as the standard deviation of the 14 m/s sample with 7°. Therefore, it can be concluded that 8 m/s are sufficient for the production of high-quality aligned fibers. Since it is not absolutely necessary to increase the rotation speed to 14 m/s and considering that 14 m/s is the absolute limit of our setup, we decided to perform the cell experiments with an 8 m/s sample. We have also discussed this in detail in the manuscript. It seems that the measured fiber diameter increases with the rotational speed. However, in this work we did not investigate this behavior in more detail. If you take a closer look at the shape of the fibers at higher speeds, it seems that the shape becomes more and more ribbon-like. The*

increase in diameter can therefore possibly also be attributed to flattening of the fibers. Investigations in this direction would certainly be relevant in future work. We have also discussed this in the manuscript.

Comment #8: How was the directionality of cells determined? Was it based on the long axis of the cells?

Author response: *The directionality of the cells was determined with the same method used for the analysis of the fibers (i.e., a Fourier components analysis of the SEM image). Yes, the analysis was based on the long axis of the cells, which corresponds to 0° in the histograms. We clarified this in the manuscript.*

Competing Interests: No competing interests were disclosed.

Reviewer Report 21 August 2024

https://doi.org/10.21956/openreseurope.19906.r43363

© 2024 Luksch H. This is an open access peer review report distributed under the terms of the Creative Commons Attribution License, which permits unrestricted use, distribution, and reproduction in any medium, provided the original work is properly cited.

Harald Luksch
Technische Universität München, Weihenstephan, Germany

The authors have responded well to my comments, and added additional figures to indicate the alignment statistics of the fibers. In addition, the expansion of the introduction and the overall presentation has improved the manuscript. I see no further necessity for additional changes.

Is the rationale for developing the new method (or application) clearly explained?
Partly

Is the description of the method technically sound?
Partly

Are sufficient details provided to allow replication of the method development and its use by others?
Partly

If any results are presented, are all the source data underlying the results available to ensure full reproducibility?
Partly

Are the conclusions about the method and its performance adequately supported by the findings presented in the article?

Partly

Competing Interests: No competing interests were disclosed.

Reviewer Expertise: Neuroscience, in-vitro studies of nervous system, neurophysiology, neuroanatomy.

I confirm that I have read this submission and believe that I have an appropriate level of expertise to confirm that it is of an acceptable scientific standard.

Version 1

Reviewer Report 27 June 2024

https://doi.org/10.21956/openreseurope.18773.r40815

© 2024 Vieira S et al. This is an open access peer review report distributed under the terms of the Creative Commons Attribution License, which permits unrestricted use, distribution, and reproduction in any medium, provided the original work is properly cited.

?

Sandra I. Vieira
Institute of Biomedicine (iBiMED) research unit - Department of Medical Sciences, University of Aveiro, Aveiro, Portugal
Nathalie Barroca
TEMA research unit - Department of Mechanic Engineering, University of Aveiro, Aveiro, Aveiro, Portugal

Lifka et al. here present two methods for structuring surfaces aiming to improve the alignment of cells like Schwann cells, important for aiding the oriented growth of neuronal axons during peripheral nervous system regeneration. The methods are generally sound and the Zenodo repository associated with this article has examples of various of the steps taken and calculations performed. The authors cultured mouse Schwann cells for one week on top of the aligned nanofibers and PET nanoripples, which appear to have induced cell alignment. It is particularly visible the influence of the nanorippled topography as an external stimulus that renders the Schwann cells' alignment.

The Introduction section has some relevant reported data, but nothing on the biological problem that authors aim to tackle, which should not only be addressed in the Abstract (attention that PNI regeneration is not that ineffective – only in 'large defects'). To better contextualize the need for the here-developed biomaterials, authors should include a short characterization of the PNS regeneration process, including the role of Schwann cells in bands of Bungner, in the Introduction section. This is necessary to support the author's Conclusion that the alignment of Schwann cells may subsequently lead to better axonal regeneration. As for the manufacturing technologies, the introduction should also contextualize better the current state of the art regarding the exploitation of electrospinning and LIPSS, to highlight their relevance for repairing strategies for

the PNS. For instance, the direct laser patterning technique has been already used to fabricate nanoripples and dual-rough hierarchical micro/nano structures to control Schwann cells attachment and migration. [Refer ref 1].
Also, since nano-structuring is known for both boosting and inhibiting cell functions, this should be carefully explained in the introduction.

One of the methods here described applied electrospinning to create aligned polyamide nanofibers, in which a fast-rotating structured collector with a knurled surface is used, to allow the nanofibers to be effectively peeled off. Regarding the cellular alignment assay, one thing noticed is that the nanofibers of Figure 6B augmentation do not seem aligned, and authors should present a more representative zoom-in. Also, no control such as randomly aligned nanofibers, was here included for comparison purposes, and so the readers cannot visually certify the cell alignment effect. As this biomaterial is the core of this article, it would also be desirable to a) apply the same strategy as the one used in Figure 5 to have some quantitative data on cell alignment; b) perform a fluorescence microscopy analysis of e.g. the actin fibers of the cells, to complement the SEM assay.

The other method here described used a laser beam to produce grooves on the surface of a flat PET foil. It would be important that the authors showed the PET nanoripples produced by the laser beam without the presence of cells (as they did for the nanofibers in Figure 4). As nano-structuring can either promote or inhibit cell functions, nanoripples should be carefully characterized (by AFM for instance) to give readers a quantified indication of the nanostructure quality and period that promoted Schwann cells orientation. Optimum LIPSS formation should be identified. The LIPSS as a response to the laser parameters should be thoroughly explored. For instance, LIPSS in polymers can depend on the energy distribution within pulses, polarization direction, and wavelength as well as repetition rate, therefore influencing both the period and quality of the resulting nanostructures. If the authors are unable to thoroughly explore laser parameters to optimize the LIPSS formation, they should at least explain in the discussion section how they selected the current parameters and how their variation would be expected to affect the nanoripples formation.

Other issues that in our opinion should be addressed to improve the article:
- Schwann cells cultures (better subtitle) should include the cell density upon seeding on the coated biomaterials.
- The biological readout is a single one (visual analyses of SEM images) and the article would gain with other host-interaction tests, such as cell viability, proliferation and/or adhesion
-The Discussion is scarce and would gain with examples of other reported aligned nanofibers using different polymers and cues for neural cells, and by hypothesizing how could the biomaterials here presented be employed in in vivo strategies.

References

1. Yiannakou C, Simitzi C, Manousaki A, Fotakis C, et al.: Cell patterning via laser micro/nano structured silicon surfaces.*Biofabrication*. 2017; **9** (2): 025024 PubMed Abstract | Publisher Full Text

Is the rationale for developing the new method (or application) clearly explained?

Partly

Is the description of the method technically sound?

Yes

Are sufficient details provided to allow replication of the method development and its use by others?
Yes

If any results are presented, are all the source data underlying the results available to ensure full reproducibility?
Yes

Are the conclusions about the method and its performance adequately supported by the findings presented in the article?
Partly

Competing Interests: No competing interests were disclosed.

Reviewer Expertise: Sandra I. Vieira - Neuroscience, neuroregeneration and neurodegeneration, in-vitro studies of nervous system, host-biomaterials interactions. Nathalie Barroca – manufacturing of platforms for bone and neural tissue repair; electromechanical couplings in biomaterials and tissues

We confirm that we have read this submission and believe that we have an appropriate level of expertise to confirm that it is of an acceptable scientific standard, however we have significant reservations, as outlined above.

Author Response 14 Aug 2024

Sebastian Lifka

We would like to thank the reviewer for the helpful comments and suggestions on our manuscript and it is with great pleasure that we upload a revised version. To improve the quality of our paper, we revised our manuscript according to the reviewers' suggestions for improvement. Below is our detailed response to the reviewers' comments.
Comment #1: *The Introduction section has some relevant reported data, but nothing on the biological problem that authors aim to tackle, which should not only be addressed in the Abstract (attention that PNI regeneration is not that ineffective – only in 'large defects'). To better contextualize the need for the here-developed biomaterials, authors should include a short characterization of the PNS regeneration process, including the role of Schwann cells in bands of Bungner, in the Introduction section. This is necessary to support the author's Conclusion that the alignment of Schwann cells may subsequently lead to better axonal regeneration.* In the peripheral nervous system of vertebrates, neurons are responsible for receiving and transmitting electrical and chemical signals and glial cells provide the necessary support and protection for neurons. Here, the most important glial cells are Schwann cells. They are responsible for the creation of myelin sheaths that protect and insulate neuronal axons. They are also essential and indispensable for axon regeneration in the event of injury. The peripheral axons regenerate in regeneration tracks (i.e., Bünger bands) formed by elongated Schwann cells. Small gaps can regenerate from alone while large gaps are

considered to require the support of a nerve graft. But the currently proposed artificial nerve grafts have insufficient success rates, especially for large nerve gaps of several cm, and nerve autografts cause severe functional loss or risk of morbidity at the donor sites. A key factor here is the elongated orientation of the Schwann cells which is induced by stimuli from their surrounding either in the extra cellular matrix or in case of artificial implants by the supporting material. We have added these considerations in a new paragraph at the beginning of the section Introduction with the new reference Manganas et al., 2022.

Comment #2: *As for the manufacturing technologies, the introduction should also contextualize better the current state of the art regarding the exploitation of electrospinning and LIPSS, to highlight their relevance for repairing strategies for the PNS. For instance, the direct laser patterning technique has been already used to fabricate nanoripples and dual-rough hierarchical micro/nano structures to control Schwann cells attachment and migration. [Refer ref 1]. Also, since nano-structuring is known for both boosting and inhibiting cell functions, this should be carefully explained in the introduction.*

We have added two new paragraphs in the section Introduction. i.e., the second and the third, with more details on the state of the art regarding the exploitation of electrospinning and LIPSS for nerve repair graft and and control of cell growth, respectively. We refer here to the new references (Chen at., 2021; Wang et al., 2018; Kriebel et al., 2017; Wang et al., 2020; Fosodeder et al., 2020; Muck et al., 2021; Maalouf et al., 2022), as well as the reference (Yiannakou et al., 2017), which was suggested by the reviewer.

Comment #3: *Regarding the cellular alignment assay, one thing noticed is that the nanofibers of Figure 6B augmentation do not seem aligned, and authors should present a more representative zoom-in.*

Thank you very much for bringing this to our attention. We have added two new SEM images which show the underlying nanofibers in more detail. Figure 6B now shows random oriented nanofibers under the cells and Figure 6D shows the aligned nanofibers under the cells. Additionally, we performed a directionality analysis of the nanofibers under the cells. The resulting histograms show a clear orientation of the nanofibers and can be found in the Zenodo repository as extended Data (Figure S2).

Comment #4: *Also, no control such as randomly aligned nanofibers, was here included for comparison purposes, and so the readers cannot visually certify the cell alignment effect. As this biomaterial is the core of this article, it would also be desirable to a) apply the same strategy as the one used in Figure 5 to have some quantitative data on cell alignment; b) perform a fluorescence microscopy analysis of e.g. the actin fibers of the cells, to complement the SEM assay.*

As already requested by Reviewer 1, we applied the same analysis methods as for the oriented nanofibers to the cells and included the resulting histograms in the manuscript. In addition, we performed fluorescence microscopy of cells on nanofibers (on flat cover glass surface, randomly oriented, and aligned) and on a flat cover glass as control as requested. For space reasons, these images are only available in the Zenodo repository as extended data (Figure S3). The reason why we originally only analyzed SEM images was because this is the gold standard for analyzing the directionality of fibers or cells. On the other hand, the underlying fibers are not visible in fluorescence microscopy and thus it cannot be verified and shown that the cells really spread in the fiber direction.

Comment #5: *The other method here described used a laser beam to produce grooves on the surface of a flat PET foil. It would be important that the authors showed the PET nanoripples produced by the laser beam without the presence of cells (as they did for the nanofibers in Figure*

4).
We replaced one zoom-in SEM image of Figure 7 with an even more zoomed-in SEM image of the nanoripples without cells.
Comment #6: *As nano-structuring can either promote or inhibit cell functions, nanoripples should be carefully characterized (by AFM for instance) to give readers a quantified indication of the nanostructure quality and period that promoted Schwann cells orientation.*
We absolutely agree with the reviewer. These nanoripples have already been characterized in our previous work (Buchberger et al., 2023 and Heitz et al., 2024) using optical methods and AFM. The typical spatial period is about 330 nm and the height is between 110 nm and 160 nm. We have described this in more detail in the manuscript and referred to the two papers mentioned.
Comment #7: *Optimum LIPSS formation should be identified. The LIPSS as a response to the laser parameters should be thoroughly explored. For instance, LIPSS in polymers can depend on the energy distribution within pulses, polarization direction, and wavelength as well as repetition rate, therefore influencing both the period and quality of the resulting nanostructures. If the authors are unable to thoroughly explore laser parameters to optimize the LIPSS formation, they should at least explain in the discussion section how they selected the current parameters and how their variation would be expected to affect the nanoripples formation.*
In our previous work, we have investigated (for other cell types) the parameter range within one can observe “surface-induce alignment” of the cells. Within this range we saw no qualitative difference of the alignment effect. Both methods presented here provide parallel features which correspond to surface-induced alignment regime and we show here for the first time that they can be used for the orientation of Schwann cells, in deed. However, we expect no strong qualitative effect of a variation the structure size (within this regime) on the alignment. We have added these considerations in a new paragraph at the end of the section Discussion with the new references Barb et al., 2014, Barb et al., 2015, and Peterbauer et al., 2010.
Comment #8: *Schwann cells cultures (better subtitle) should include the cell density upon seeding on the coated biomaterials.*
The cell density upon seeding was 25,000 cells per cm2 resulting in a total number of approximately 65,000 cells per sample. We added this to the cell cultivation subsection in the manuscript.
Comment #9: *The biological readout is a single one (visual analyses of SEM images) and the article would gain with other host-interaction tests, such as cell viability, proliferation and/or adhesion.*
We can understand the reviewer's view, but we are currently still struggling with our methods to determine cell adhesion, as the samples used here are very flexible and therefore cannot be measured reliably with our methods. Furthermore, when determining viability and proliferation, we see the problem that our samples are structured and therefore have a significantly different surface size than a flat control sample, which in our opinion makes the evaluation difficult and not very meaningful. A single cell analysis might be possible, but it is difficult and extremely imprecise. As this article focuses on a method for directional growth of Schwann cells, we have refrained from determining additional parameters.
Comment #10: *The Discussion is scarce and would gain with examples of other reported aligned nanofibers using different polymers and cues for neural cells, and by hypothesizing how could*

the biomaterials here presented be employed in in vivo strategies.
We see the point of the reviewer, but we think we have addressed it already in the description of the state of the art in the second paragraph of the section Introduction (see above).

Competing Interests: No competing interests were disclosed.

Reviewer Report 08 June 2024

https://doi.org/10.21956/openreseurope.18773.r40812

© 2024 Luksch H. This is an open access peer review report distributed under the terms of the Creative Commons Attribution License, which permits unrestricted use, distribution, and reproduction in any medium, provided the original work is properly cited.

?

Harald Luksch
Technische Universität München, Weihenstephan, Germany

In their submission entitled “Oriented artificial nanofibers and laser induced periodic surface structures as substrates for Schwann cells alignment”, Lifka and colleagues describe a way of structuring surfaces for better orientation of biological cells. Such orientation might be helpful for oriented growth of neurons in, e.g, regeneration processes after injuries to the peripheral nervous system.
Lifka et al use two different methods for structuring the surface, namely the production of grooves with a laser beam, or the production of a nanofiber mat with electrospun polyamide nanofibers. For the latter process, a key feature of the spinning process was improved by using a fast rotating structured collector with a knurled surface. The woven nanofiber mat can be removed without damage or residual material attached to the collector. Both the mat and the laser-fabricated grooves were inspected with Scanning Electron Microscopy and showed well aligned fibers or grooves, respectively.
The authors then cultivated mouse Schwann cells from a cell line onto either substrate for a week, and analysed the orientation of the cells and their processes. From the images provides in the submission, a clear influence of the structure on the cellular orientation is evident. However, a quantitative assessment of cell orientation in both the control cultures and the cultures on structured surfaces would have been good, to clearly show the orientation and to quantify the effect of the given structure. After all, the parameters chosen for either structuring method might be suboptimal, and variations of the structures (i.e., deeper or wider grooves etc.) might lead to even better orientation control. The authors conclude that their production of mechanical nanofeatures is capable of influencing glial cells into an oriented growth, and thus may potentially aid axonal regeneration.
My impression is that this report is a valuable addition to manufacturing processes for structured surfaces for nerve regeneration. The method description is sound, the images illustrate the respective issues well, and the conclusions are well founded.

Is the rationale for developing the new method (or application) clearly explained?

Yes

Is the description of the method technically sound?
Yes

Are sufficient details provided to allow replication of the method development and its use by others?
Yes

If any results are presented, are all the source data underlying the results available to ensure full reproducibility?
Yes

Are the conclusions about the method and its performance adequately supported by the findings presented in the article?
Partly

Competing Interests: No competing interests were disclosed.

Reviewer Expertise: Neuroscience, in-vitro studies of nervous system, neurophysiology, neuroanatomy.

I confirm that I have read this submission and believe that I have an appropriate level of expertise to confirm that it is of an acceptable scientific standard, however I have significant reservations, as outlined above.

Author Response 14 Aug 2024

Sebastian Lifka

We would like to thank the reviewer for the helpful comments and suggestions on our manuscript and it is with great pleasure that we upload a revised version. To improve the quality of our paper, we revised our manuscript according to the reviewers' suggestions for improvement. Below is our detailed response to the reviewers' comments.
Comment #1: *From the images provides in the submission, a clear influence of the structure on the cellular orientation is evident. However, a quantitative assessment of cell orientation in both the control cultures and the cultures on structured surfaces would have been good, to clearly show the orientation and to quantify the effect of the given structure.*
Thank you very much for that valuable input, we added a figure (Figure 8) where we analyzed the directionality of the cells on the nanofibers (random oriented and aligned) and on the PET foils (flat and with nanoripples) using the same method as for the analysis of the aligned nanofibers. The resulting histograms show a clear orientation of the cells on aligned nanofibers and nano-structured PET foils.
Comment #2: *After all, the parameters chosen for either structuring method might be suboptimal, and variations of the structures (i.e., deeper or wider grooves etc.) might lead to even better orientation control.*
In our previous work, we have investigated (for other cell types) the parameter range within

one can observe “surface-induce alignment” of the cells. Within this range we saw no qualitative difference of the alignment effect. Both methods presented here provide parallel features which correspond to surface-induced alignment regime and we show here for the first time that they can be used for the orientation of Schwann cells, in deed. However, we expect no strong qualitative effect of a variation the structure size (within this regime) on the alignment. We have added these considerations in a new paragraph at the end of the section Discussion with the new references Barb et al., 2014, Barb et al., 2015, and Peterbauer et al., 2010.

Competing Interests: No competing interests were disclosed.